응집물리(강상관 전자계) 관점에서 바라본

Resonant Inelastic X-ray Scattering

공명 비탄성 엑스선 산란

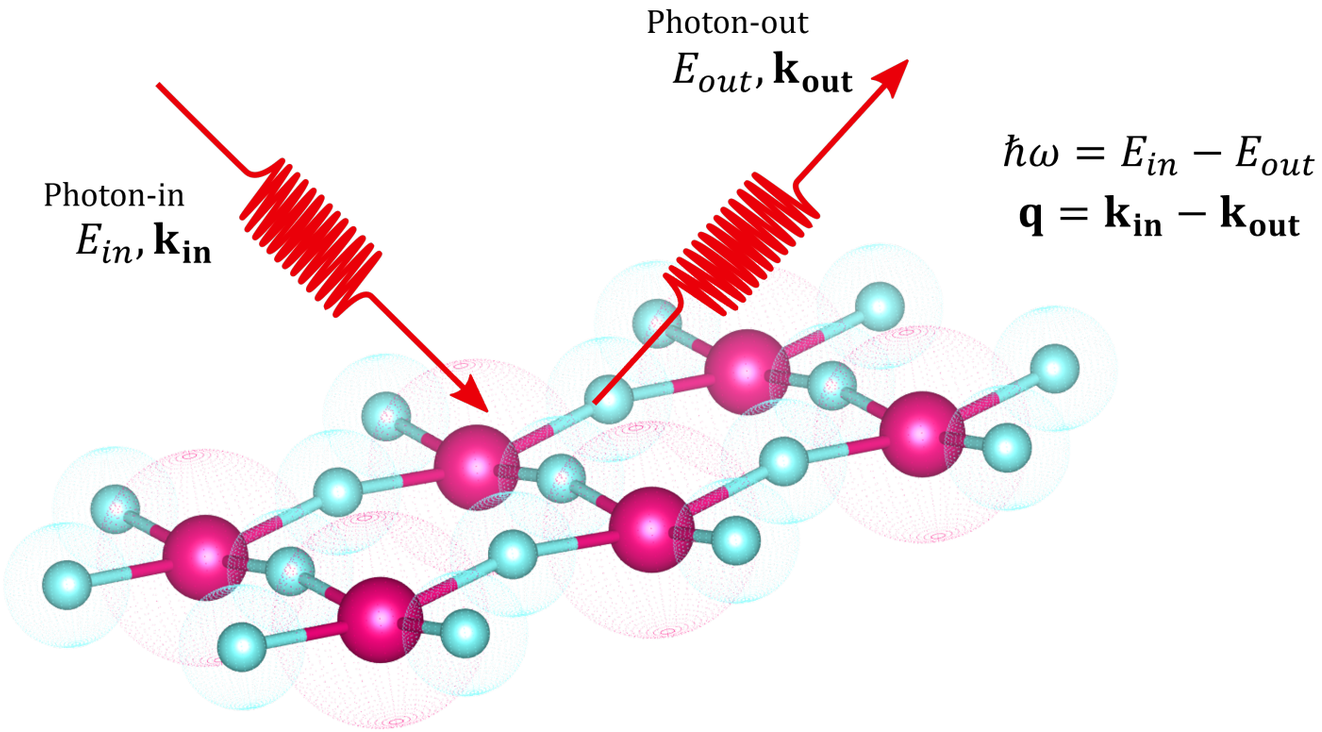

2024 가속기 및 빔라인 미래인재 양성 교육단 여름학교
07. 10. 2024

김범준
포항공대 (POSTECH)

Elastic vs. Inelastic

=diffraction

Static vs. Dynamic

structure factor $S(q)$ $S(q, \omega)$ dynamic structure factor

$q = k_f - k_i$ momentum transfer

$\hbar\omega = E_f - E_i$ energy transfer

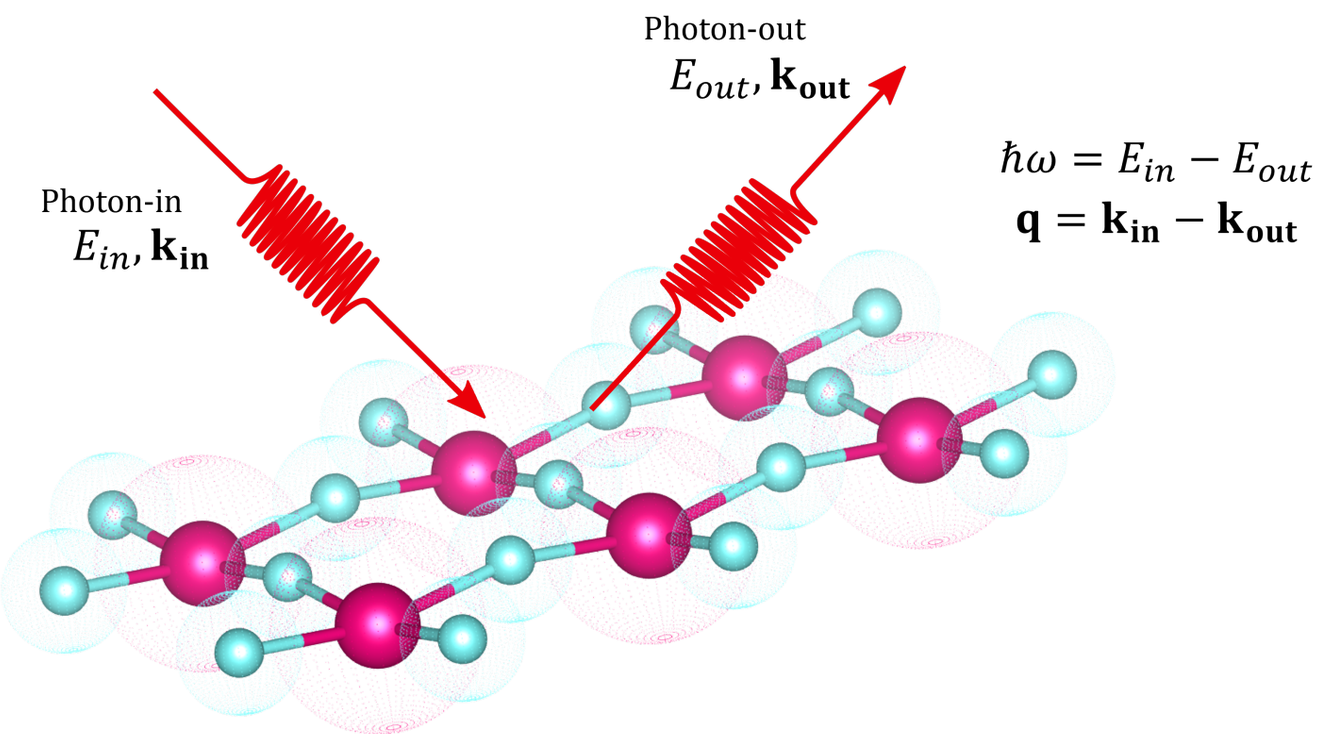

X-ray vs. Neutron

EM wave

neutral, S=1/2

electromagnetic force

strong force,
magnetic dipole interaction

phonon dispersion
magnon dispersion

structure factor $S(q)$

$$= \int \rho(r) e^{-iq \cdot r} dr$$

$S(q, \omega)$ dynamic structure factor

$q = k_f - k_i$ momentum transfer

$\hbar\omega = E_f - E_i$ energy transfer

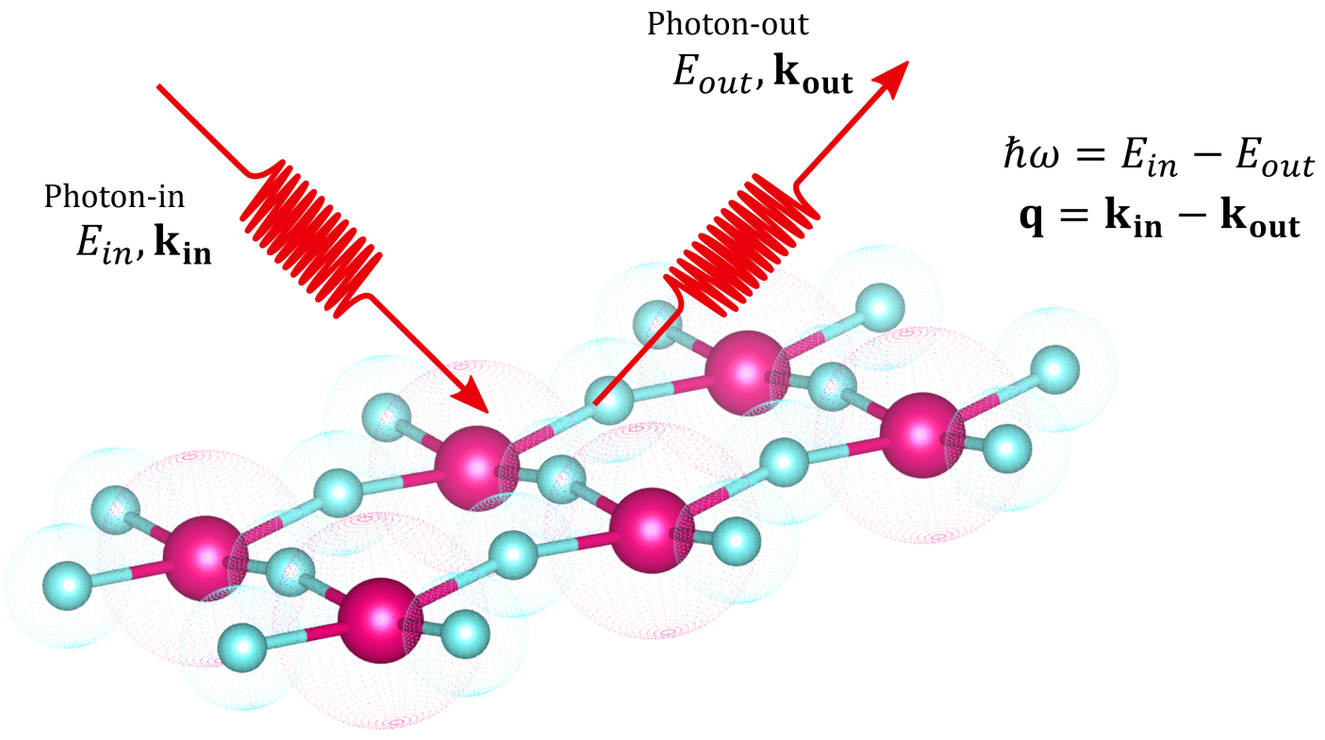

Resonance

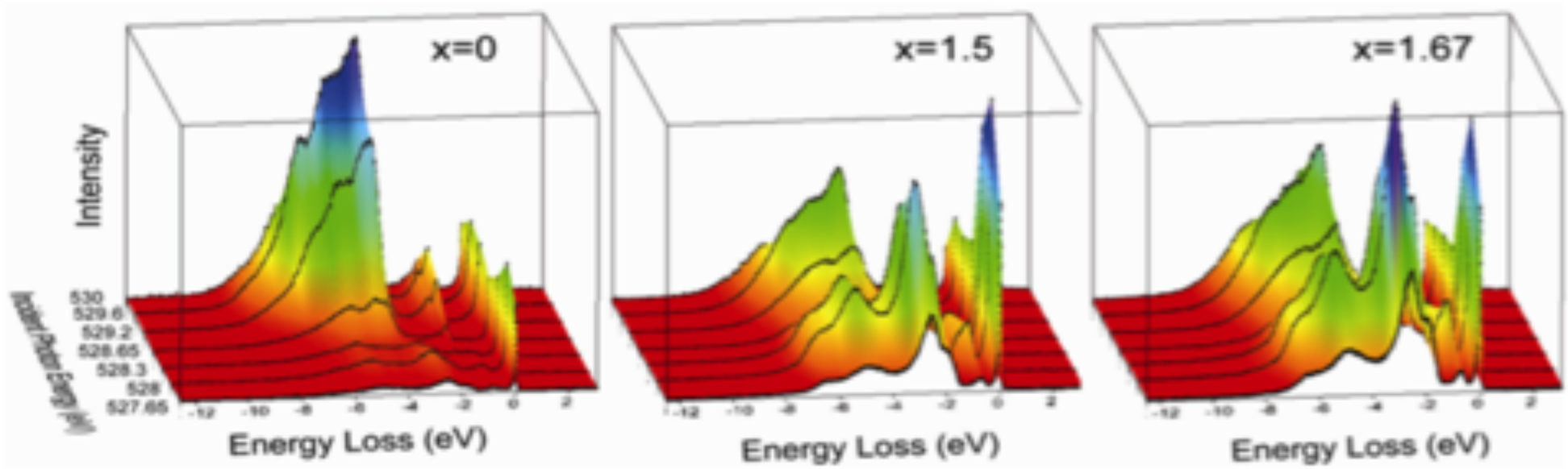

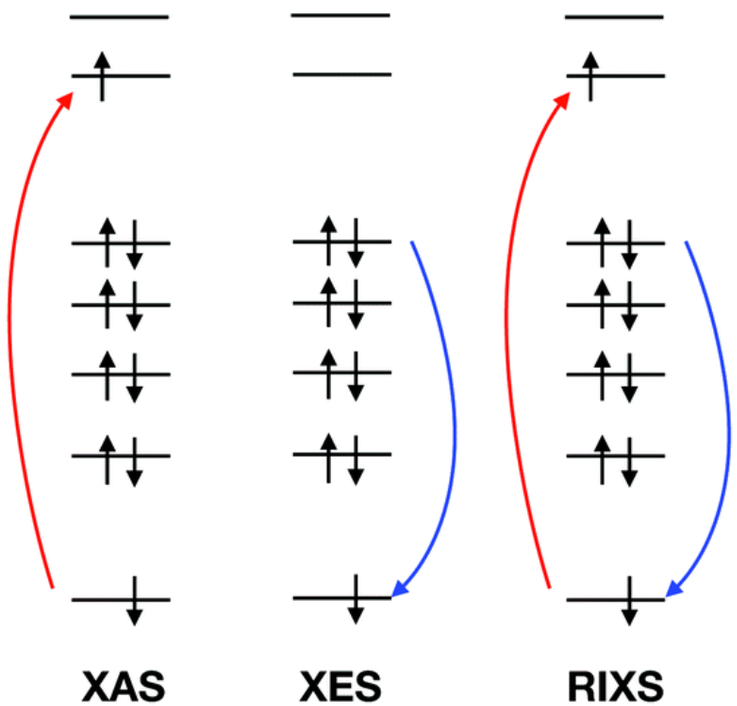

X-ray absorption spectroscopy (XAS)

X-ray emission spectroscopy (XES)

Resonant inelastic X-ray scattering

=XAS (absorption) +XES (emission)

X-ray Absorption Spectroscopy

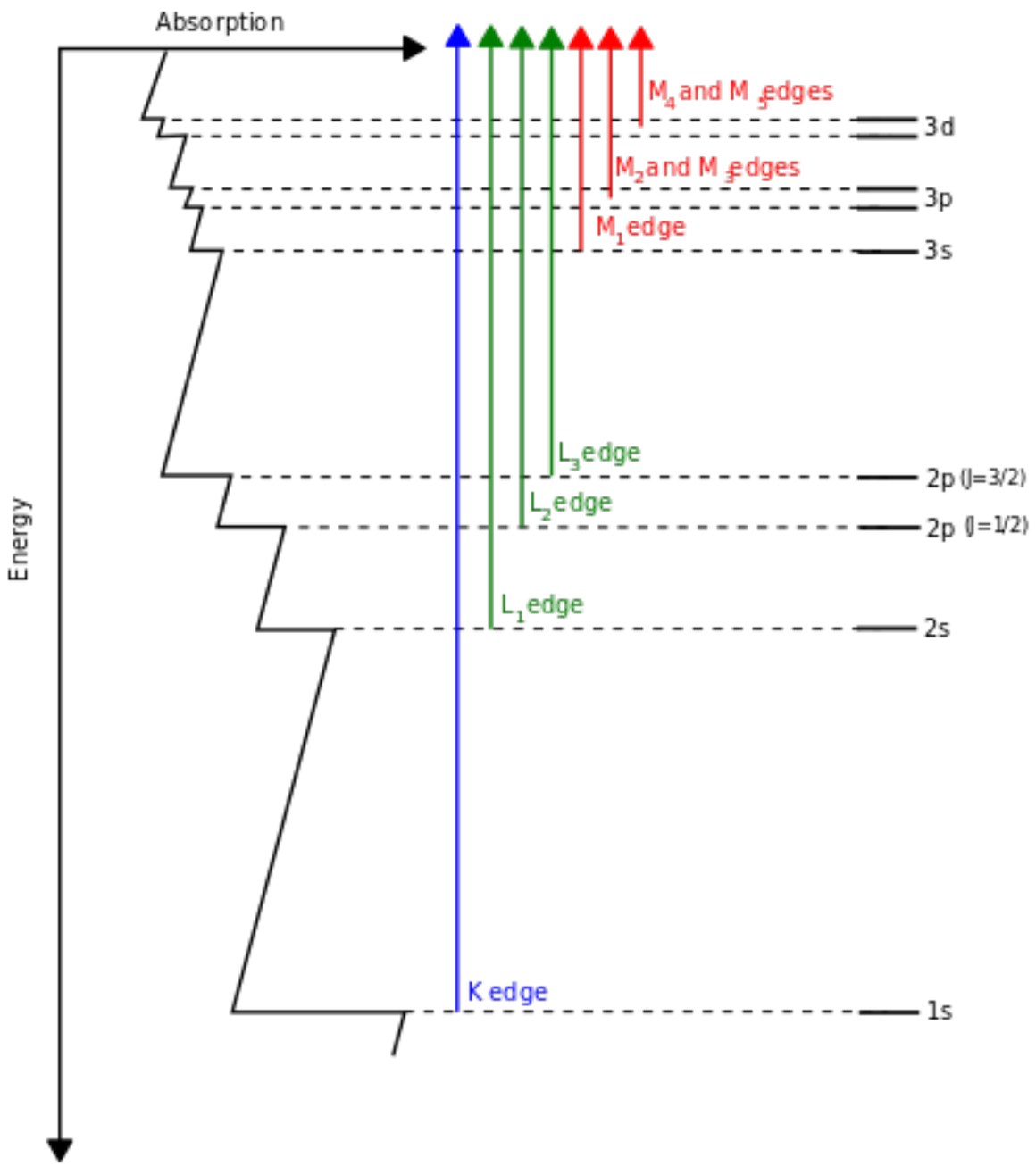

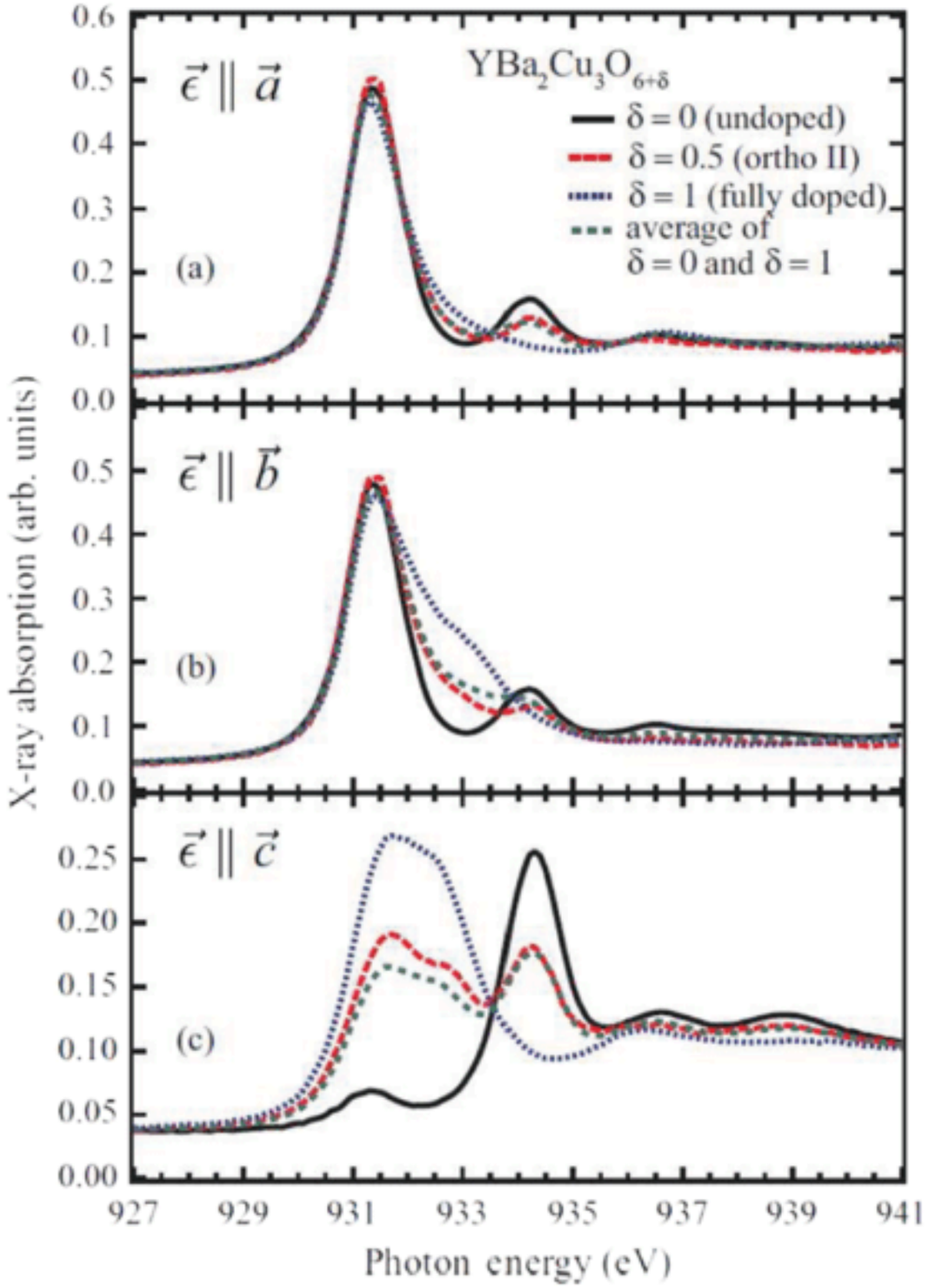

Resonance

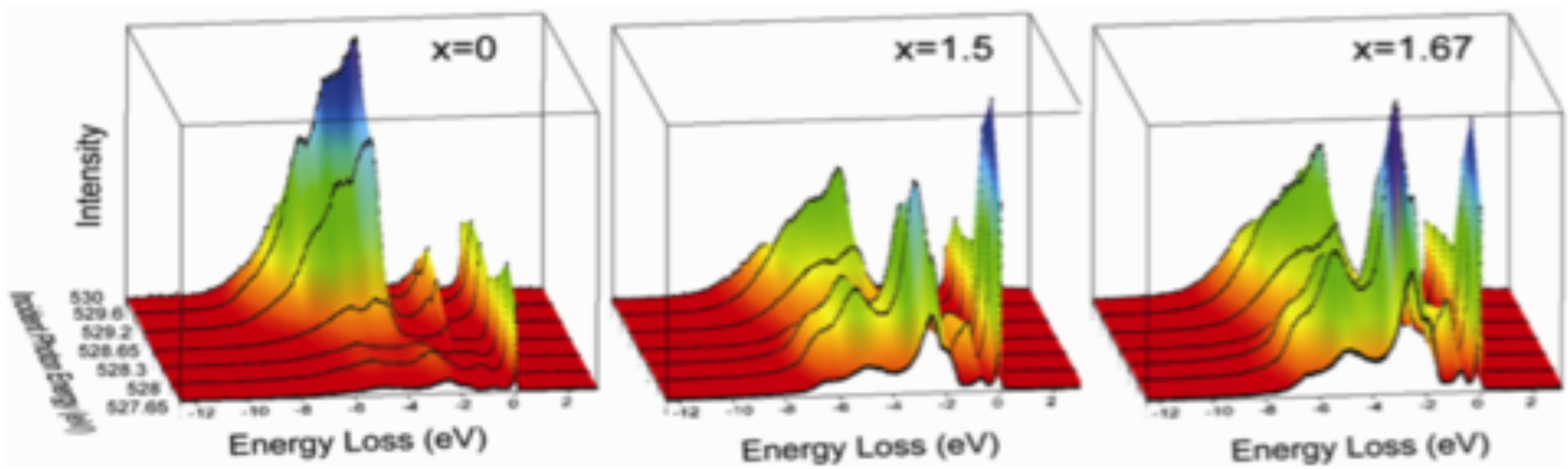

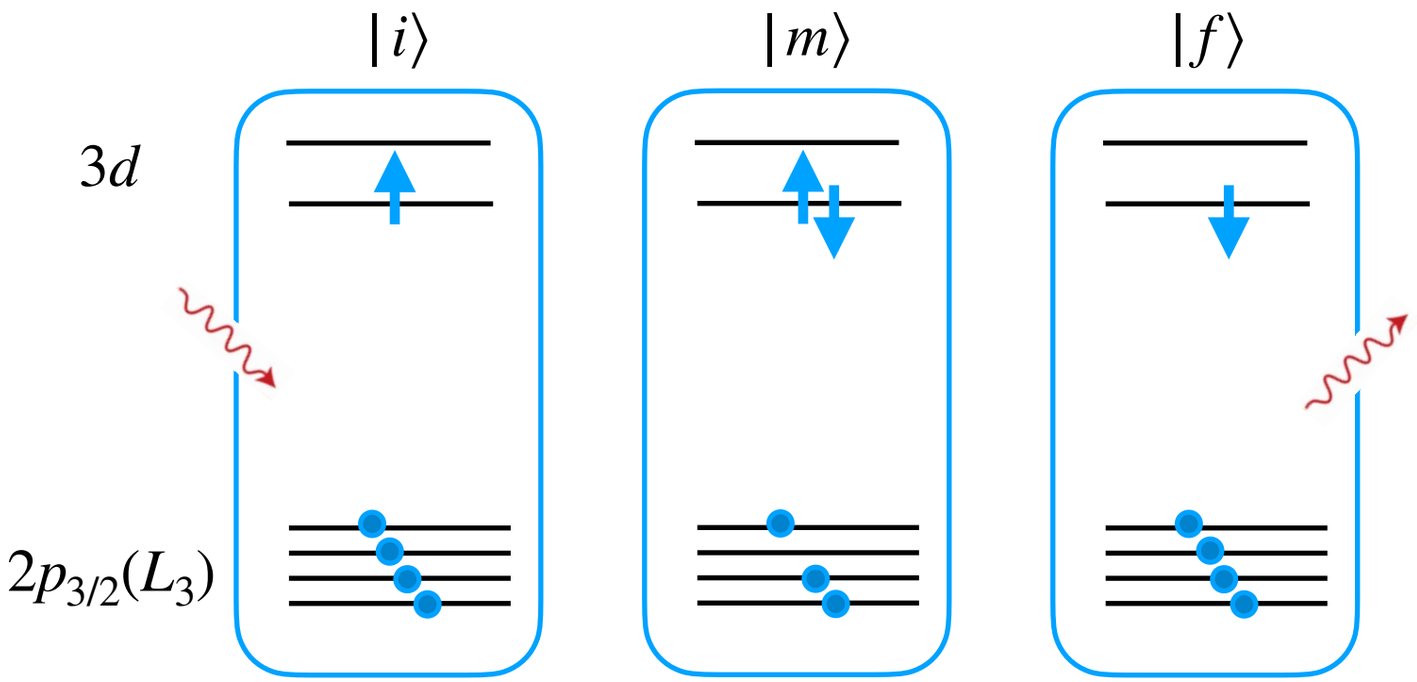

spin excitation

orbital excitation

charge excitation

lattice excitation

Resonance

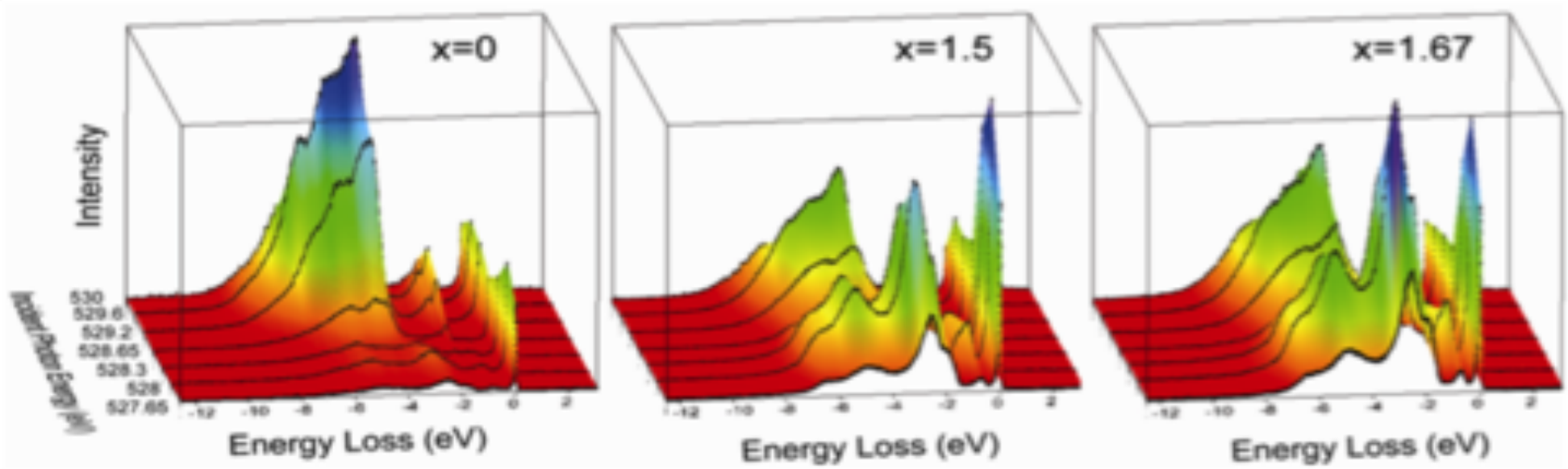

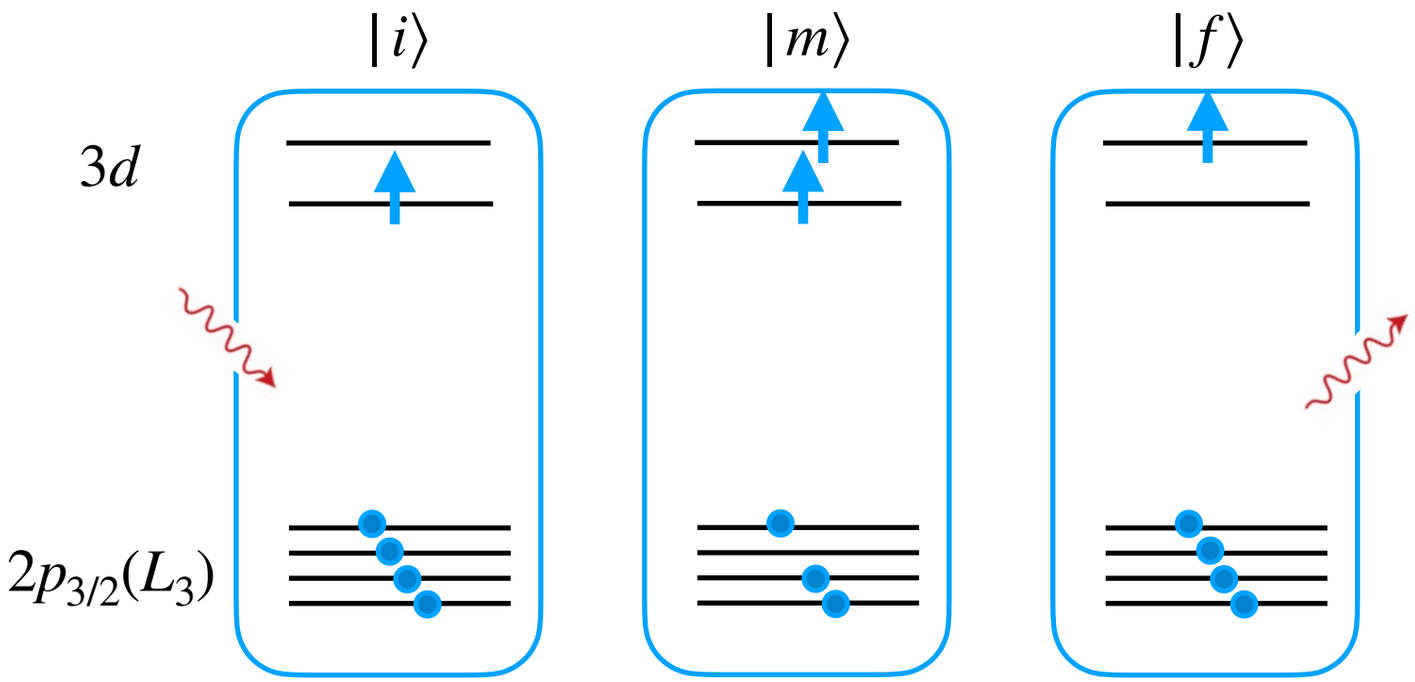

spin excitation

orbital excitation

charge excitation

lattice excitation

Resonant inelastic x-ray scattering

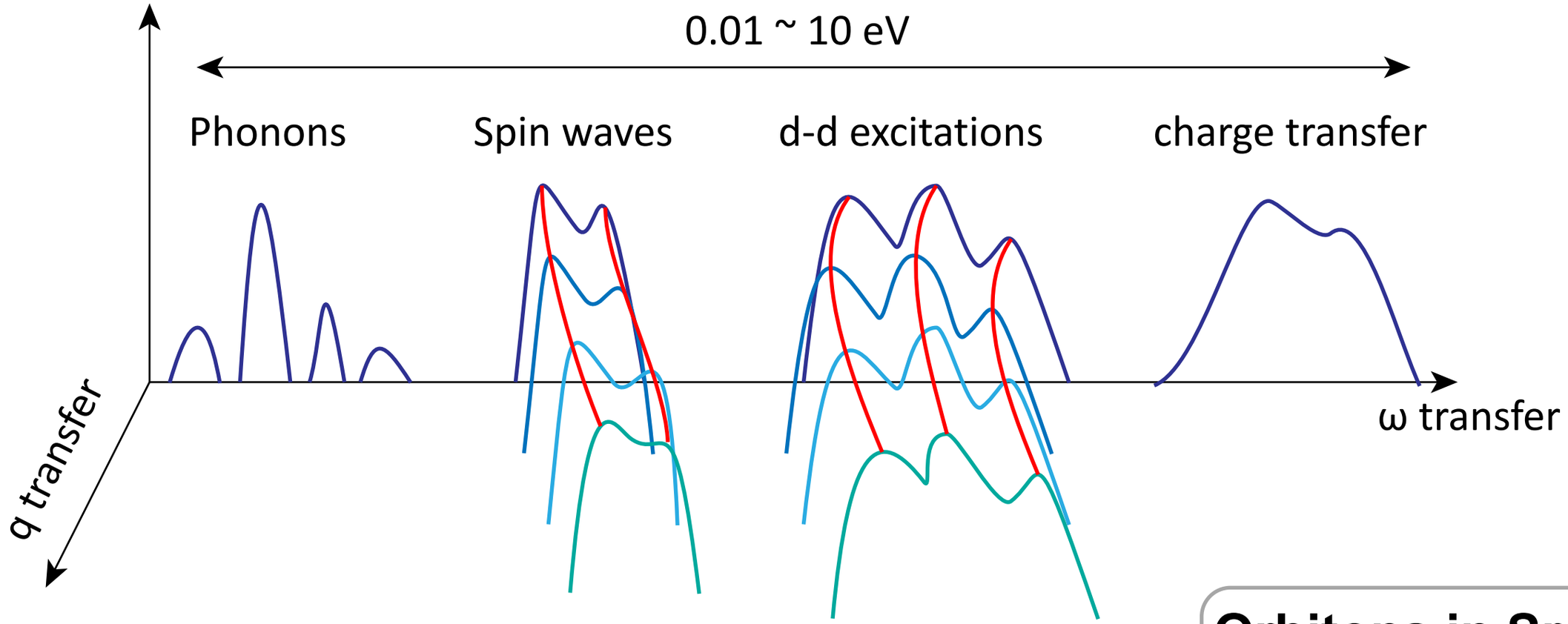

Phonons in CuO

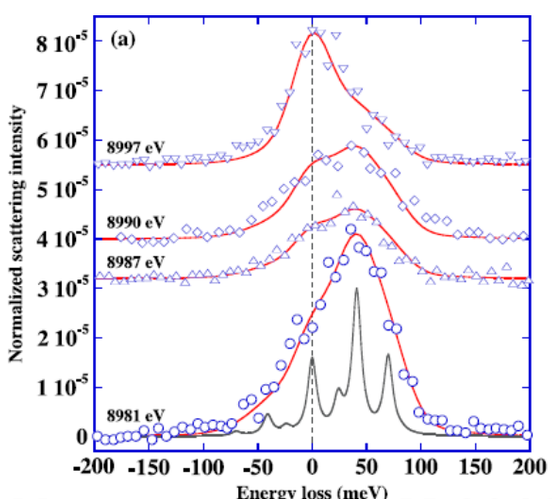

Yavas et al. JPCM 2010

Magnon in La_2CuO_4

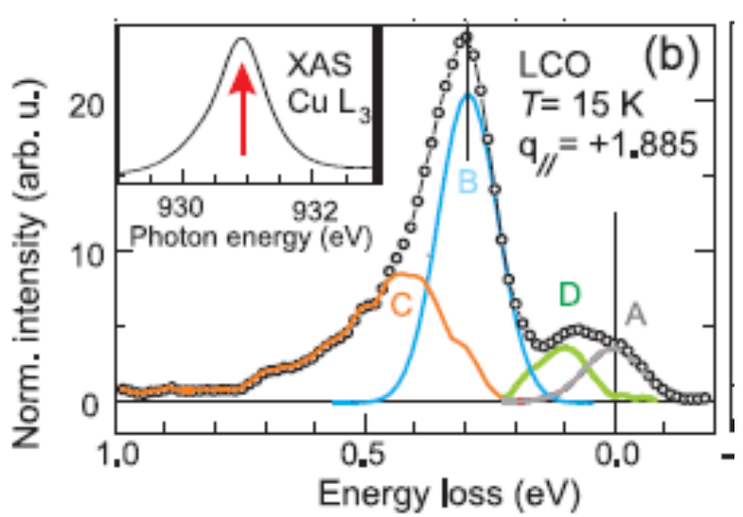

Braicovich et al. PRL 2010

Orbitons in Sr_2CuO_3

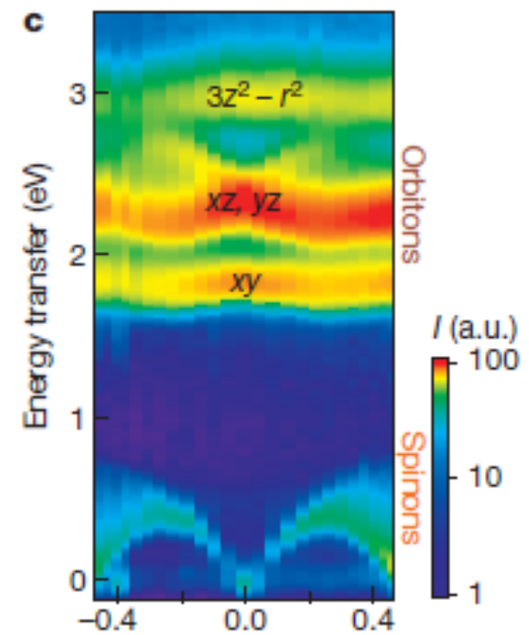

Schlappa et al. Nature 2012

RIXS

S(q,ω)

dynamic structure factor

INS

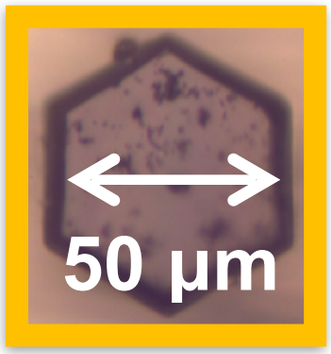

tiny crystals

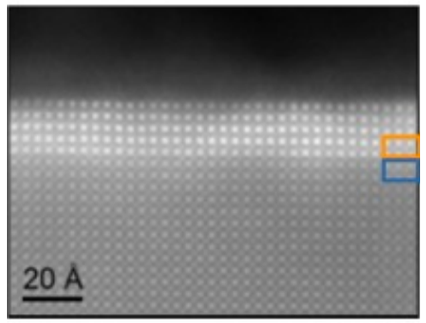

thin films

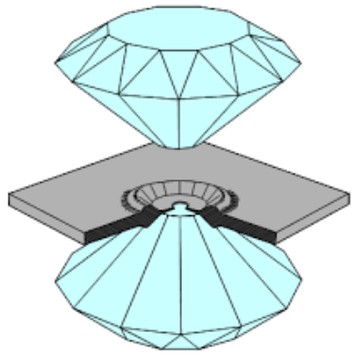

high pressure

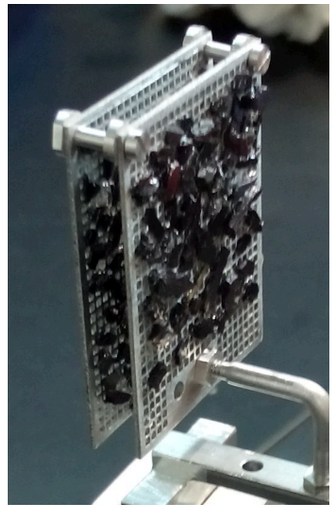

Sr_2IrO_4

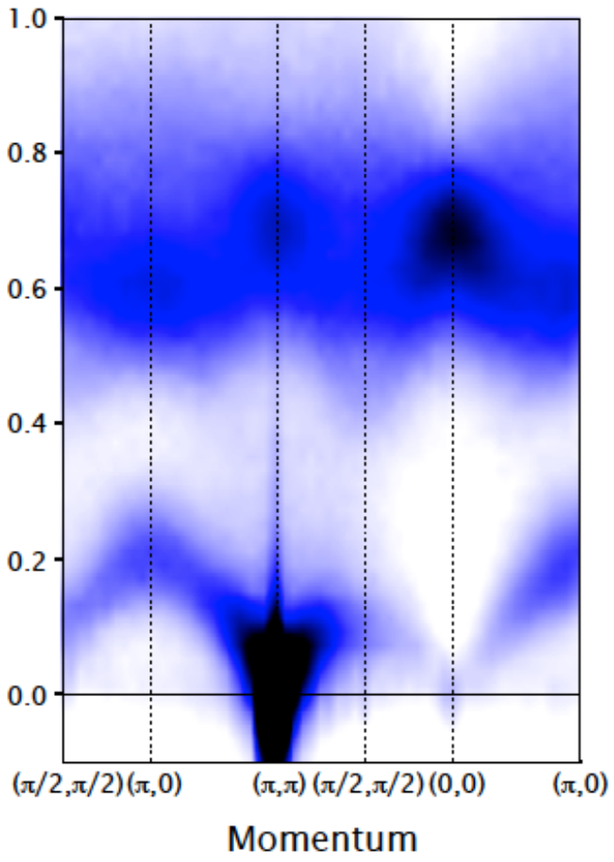

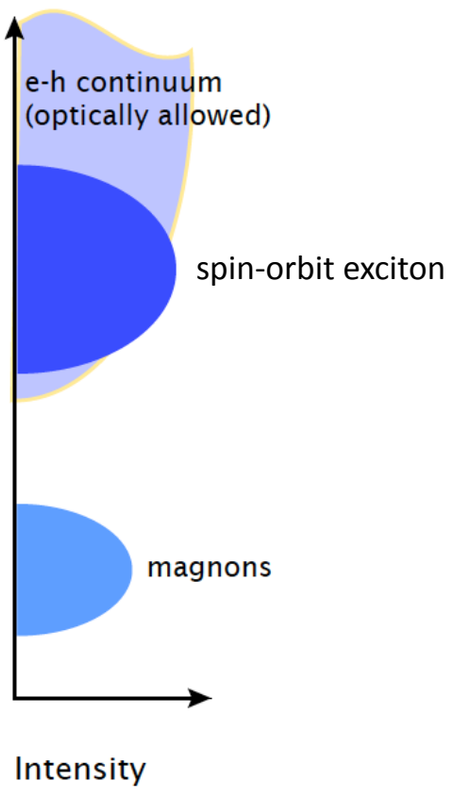

J. Kim & BJK et al. PRL (2012)

Ca_2RuO_4

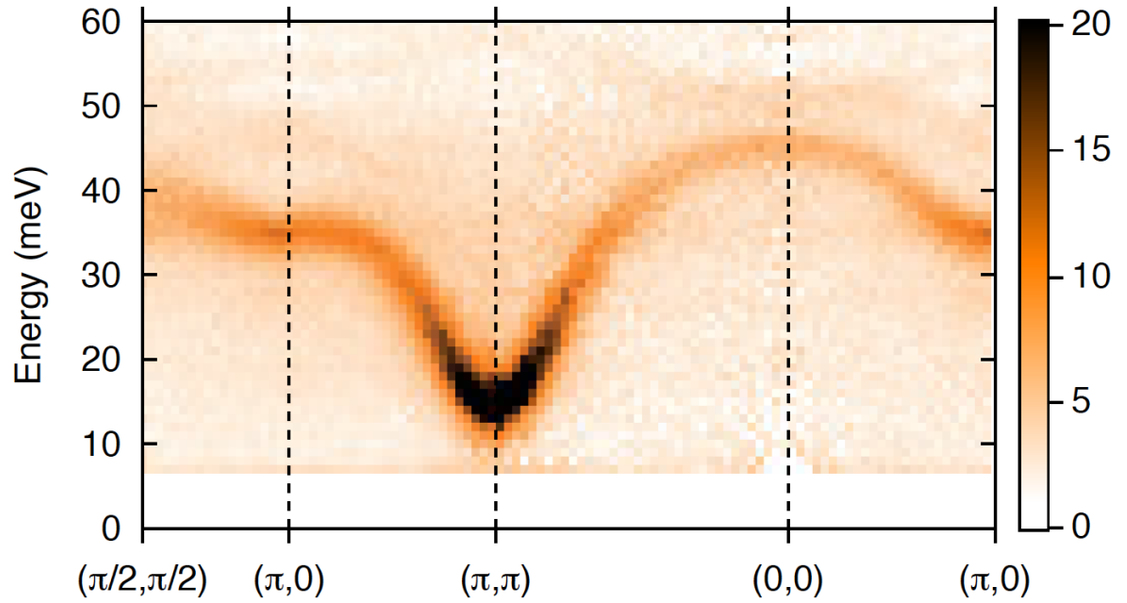

A. Jain & BJK et al. Nature Phys. (2017)

Brief history

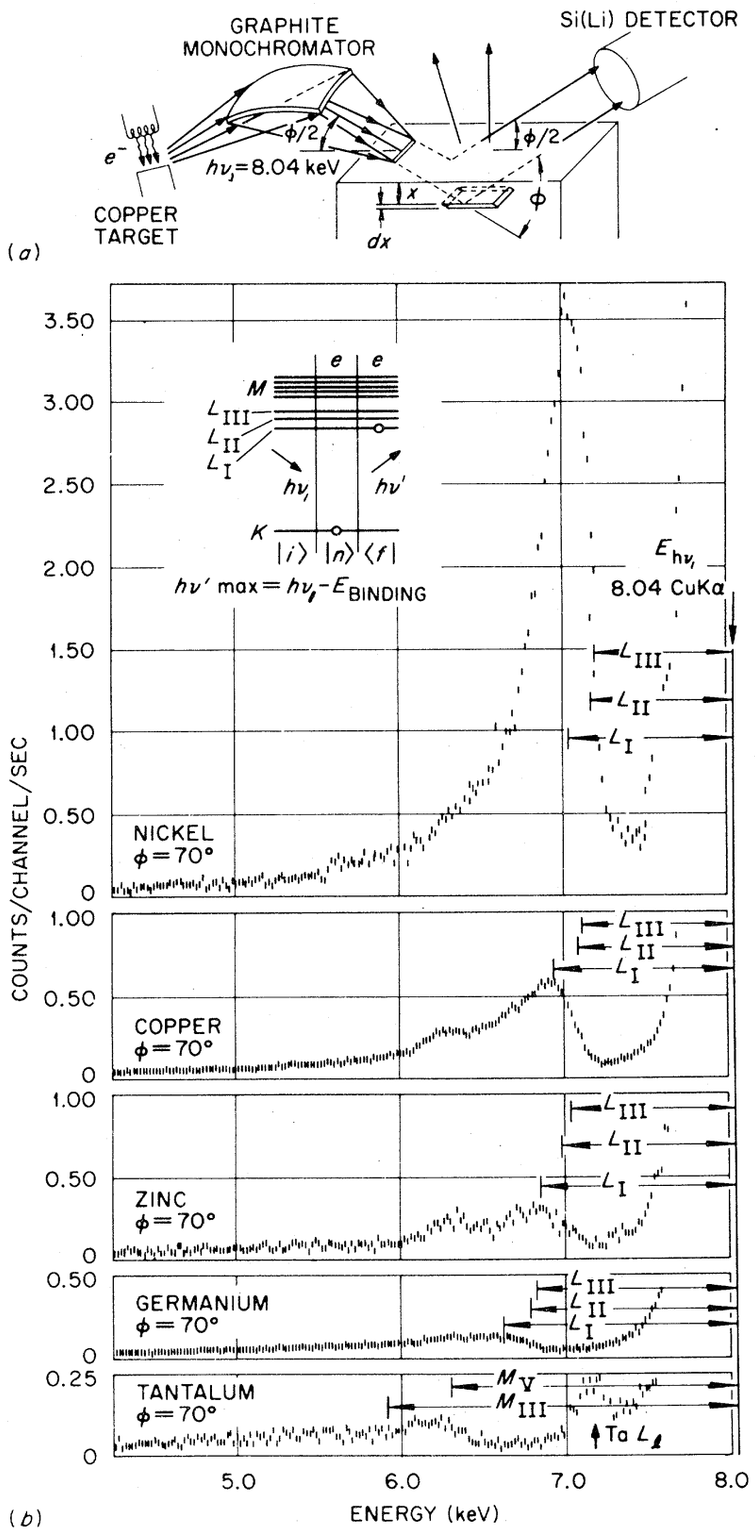

VOLUME 33, NUMBER 5 PHYSICAL REVIEW LETTERS 29 JULY 1974

Inelastic Resonance Emission of X Rays: Anomalous Scattering Associated with Anomalous Dispersion*

Cullie J. Sparks, Jr.
Metals and Ceramics Division, Oak Ridge National Laboratory, Oak Ridge, Tennessee 37830
(Received 13 May 1974)

190 eV resolution @ 5.9 keV

ing increases rapidly in intensity. The cross section for the observed scattering is shown to be predicted by the $\vec{P}\cdot\vec{A}$ term in second-order perturbation theory, a term previously neglected in inelastic x-ray scattering calculations.

Brief history

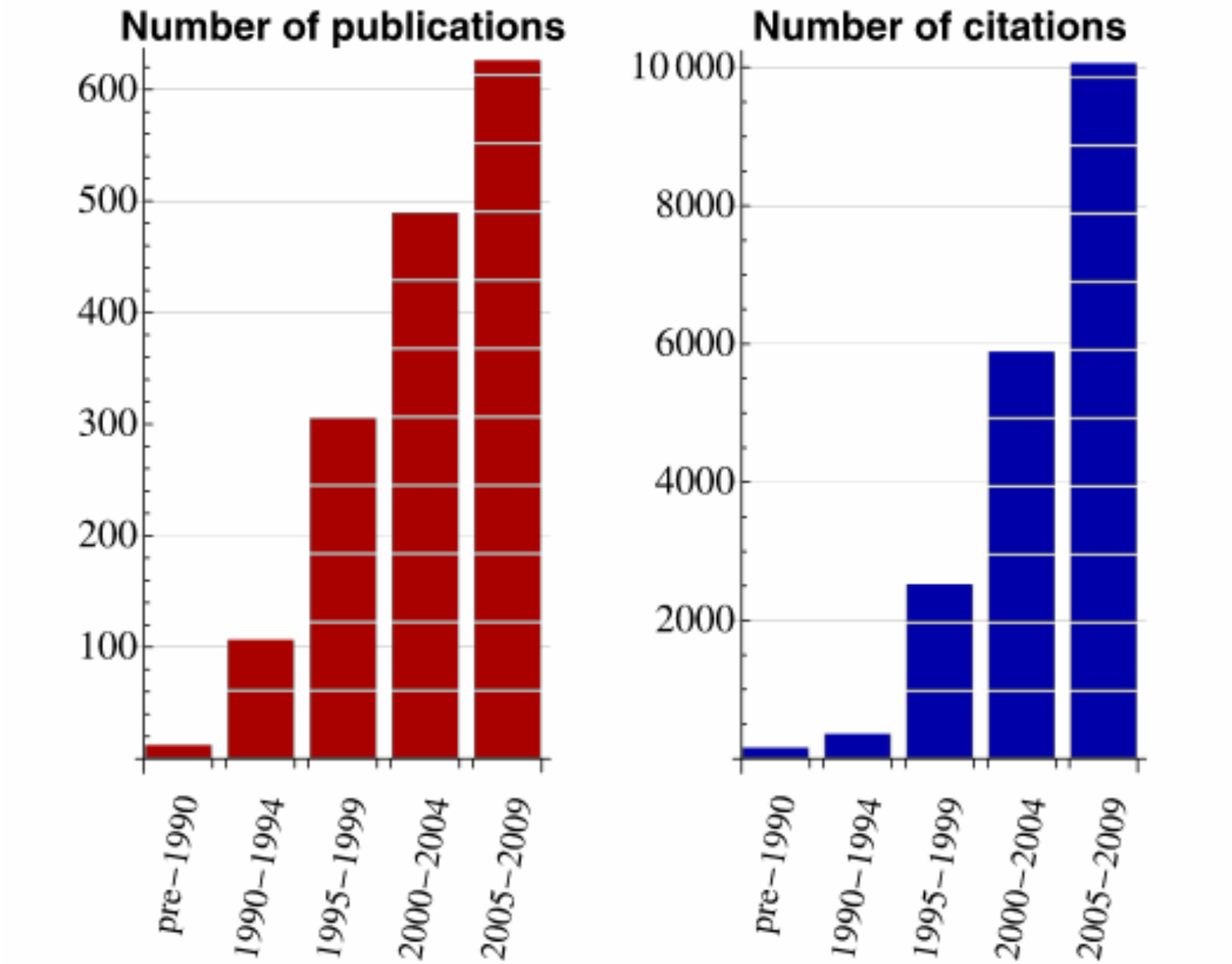

L. Ament et al., Rev. Mod. Phys. 83, 705 (2011)

Brief history

2017: <10 meV
2012: 25 meV

Ir L3 edge 11.2 keV
resolving power >10^6

2010: 130 meV, 3000 cps

2010

2007: 90 meV, 600 cps

2002: 300 meV, 6cps

1999: 1500 meV, 1cps

our first experiment on iridate (hard x-ray)
first observation of single magnon (soft x-ray)
(Braicovich & Ghiringhelli)

Magnon in La_2CuO_4

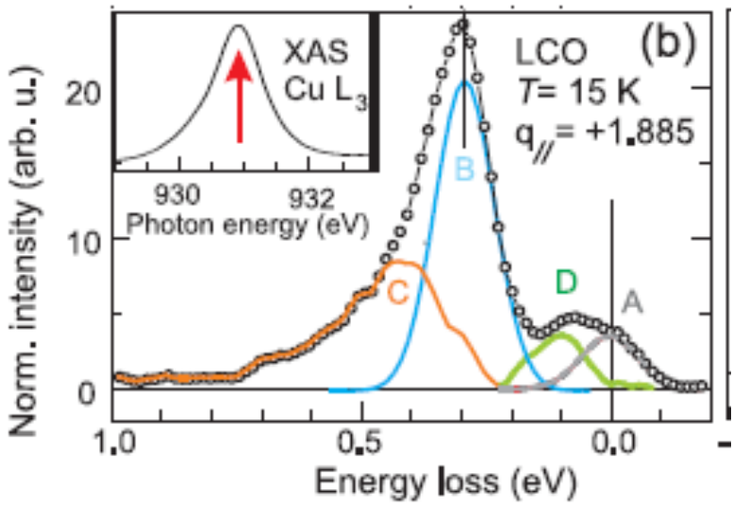

Braicovich et al. PRL 2010

L. Ament et al., Rev. Mod. Phys. (2011)

Resonant inelastic x-ray scattering

L edge

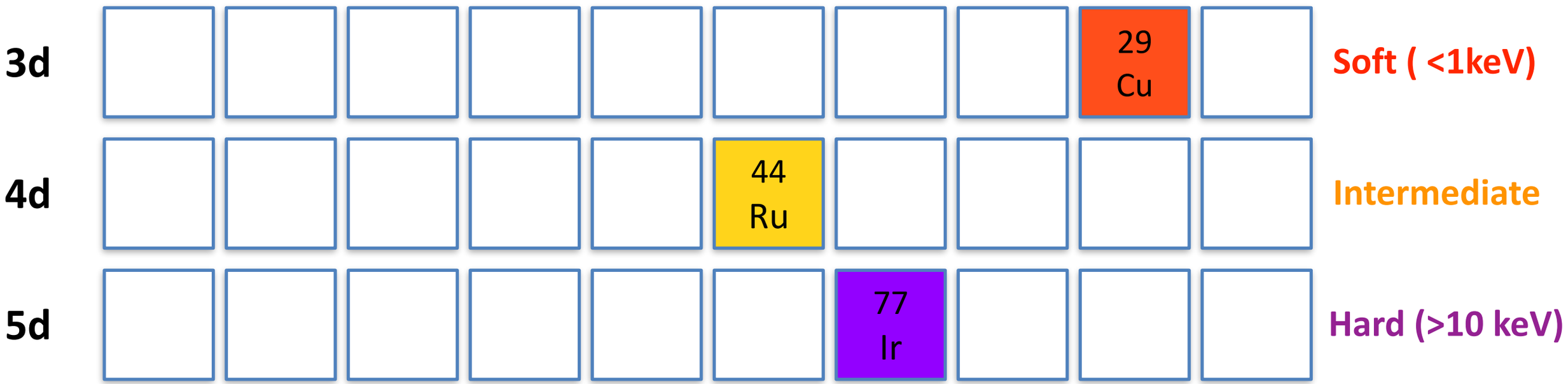

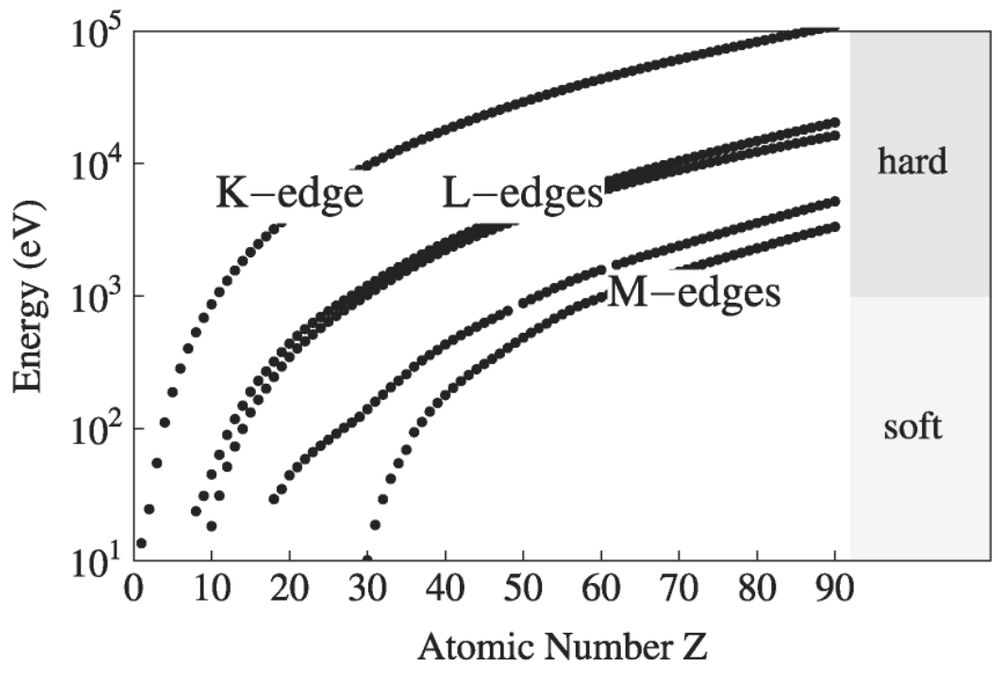

Resonant inelastic x-ray scattering

L edge

3d

Soft (<1keV)

Soft X-Ray RIXS Spectrometer at ID32, ESRF

Resonant inelastic x-ray scattering

5d

Hard (>10 keV)

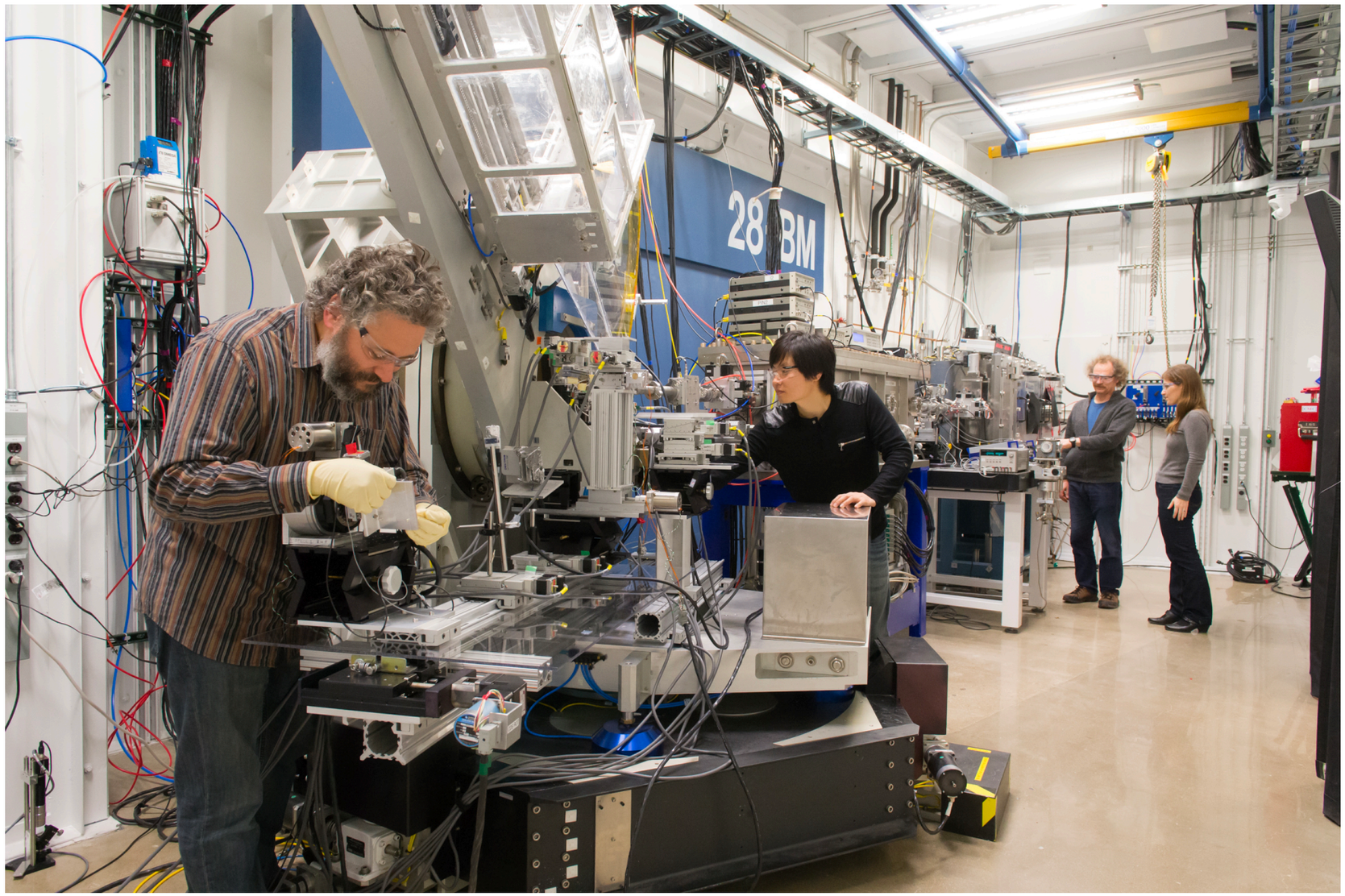

Advanced Photon Source

Argonne National Laboratory

Resonant inelastic x-ray scattering

Grating

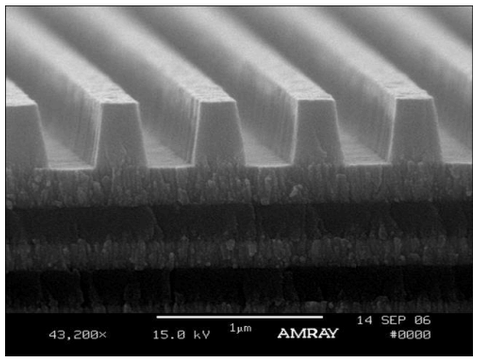

$$E = 2 \sim 3 \text{ keV}$$
$$\lambda = 0.4 \sim 0.6 \text{ nm}$$

Crystal

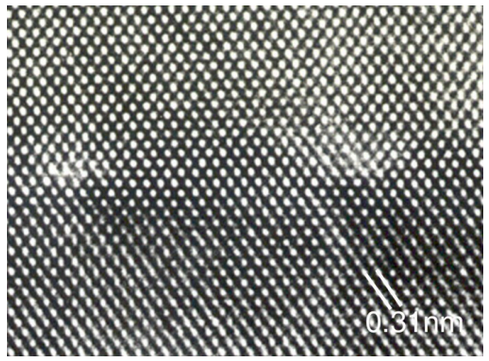

X-ray optics difficult to implement

The world's first high-resolution RIXS beamline for intermediate energy

I-RIXS project at DESY - P01 (Hamburg)

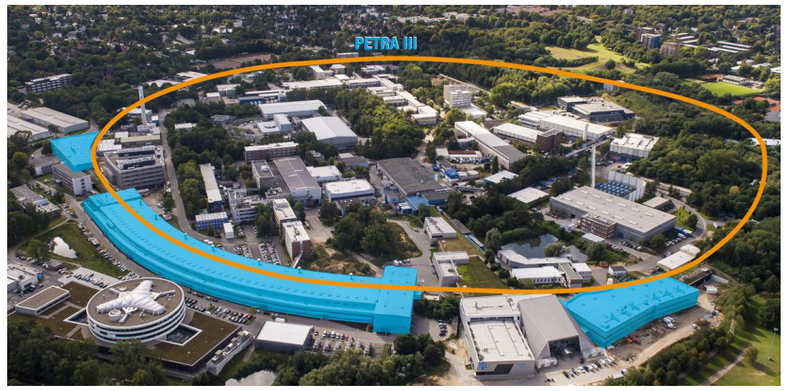

4d

					44 Ru				

Intermediate

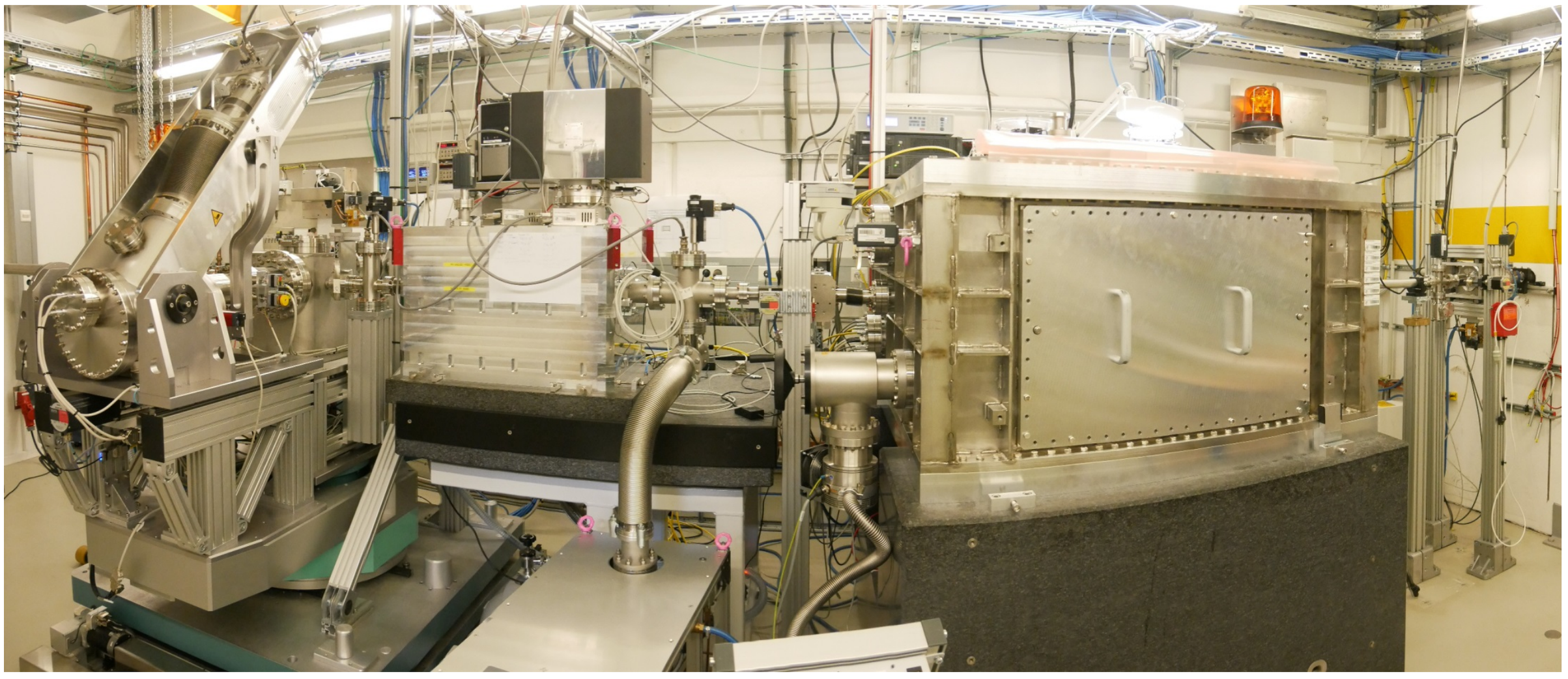

Soft x-ray RIXS beamlines

PROJECTS AROUND THE WORLD: 1

Source (country)	Scientific areas	Combined resolving power	Energy range (eV)	Time scale	Instrumentation	Contact:
ALS (USA)	Excitations in 3D materials; ultrafast phenomena	5000@ 540eV 2500@ 1keV		Spring 2016	qRIXS: time and momentum resolved RIXS	Yi-De Chaung ychuang@lbl.gov
ALS (USA)	Dispersive excitations	25000	250-1500	2017-2018	QERLIN: high throughput multiplexing for measuring dispersive excitations	Howard Padmore hapadmore@lbl.gov
BESSYII (Germany)	Solid state and molecular sciences	25000-30000	200-1500	Design finished, funded, ~2018	METRIXS: 7 m Spectrometer with momentum transfer for solid state and molecular sciences.	Alexander Föhlisch alexander.foehlisch@helmholtz-berlin.de
BESSYII (Germany)	Inhomogeneous samples	5000	100-1500	In operation	μmRIXS: PGS Spectrometer, 1μm Focus for inhomogeneous samples.	Justine Schlappa justine_schlappa@helmholtz-berlin_de
BESSYII (Germany)	Solids and molecules	3000	60-1500	In operation	flexRIXS: Compact transportable Rowland Spectrometers with dedicated solid and molecular sample environments.	Alexander Föhlisch
Diamond Light Source (UK)	Condensed matter physics, material science, strongly correlated systems,Catalysts	10000 - 40000 @ 1keV	250-3000	Installation: 2015-2016 First Light summer 2016 First Users Spring 2017.	13m scattering arm. Continuous angular rotation (150 degrees) – Cinel design. Polarization analysis. 4 collecting optics close to the sample. Can reach small forward scattering angles.	Kejin Zhou Kejin.zhou@diamond.ac.uk
MAX IV (Sweden)	Solids, Gases, liquids	>30000	250-1600	Beamline installation: Fall 2015 Spectrometer: Spring 2016. Comm.2017	10m collimating Rowland spectrometer. Detector height minimised for stability. Drift correction using zero-order. Possible future polarimeter. Continuous angular rotation over 120 degrees using differentially pumped rotation system.	Marcus Agaker marcus.agaker@physics.uu.se

Soft x-ray RIXS beamlines

PROJECTS AROUND THE WORLD: 2

NSLSII (USA)	Correlated electron systems	10000-70000	165-2300	Installation: 9/2016 1st light11/16 Users: 01/17	Piezo based diffractometer. Continuous angular rotation of 14m scattering arm with triple rotating flange system. Detector with polarimeter.	Ignace Jarrige jarrige@bnl.gov
PetraIII (Germany)	Liquids	Medium resolution	250-2300	Operational	User instrument: Possible upgrade for higher resolution	Jens Viefhaus jens.viefhaus@desy.de
Sirius (Brazil)	Gases, liquids, interfaces and solids Bio-molecules	~42000	400-1200	First Users: Beginning of 2019.	CCD detector giving a spatial resolution of 3microns. Large momentum transfer Possible rotatable platform or chamber Possibly magnetic fields	Marco Guarise marco.guarise@lnls.br
SLS (Switzerland)	Correlated Materials, Molecular physics, Chemistry/ catalysis	5800-8000 @ 930eV 7500-11800 @530eV	400 - 1700	Operational	Q rotating girder platform 30-130 degrees 6 axis manipulator from autumn 2015. 9-350K 1 inch chip CCD camera with 13.5 micron pixels From 2016 EM-CCD with 3 one inch chips and subpixel resolution around 2-3 micron Upgrade RP:13-14000 930eV New BL / spectrometer at PSI SLS 2.0 > 2020	Thorsten Schmitt thorsten.schmitt@psi.ch
Soleil (France)	Solid state-physics Liquids and gases.	5000-8000	50-950	Operational + possible new project	Electric and magnetic fields (~1T) at the sample by end 2016. Liquid and gas cells. Soleil upgrade project 2020? High resolution (>20000) 8m long spectrometer.	Nicolas Jaouen nicolas.jaouen@synchrotron-soleil.fr
SSRF (China)	Electronic structure of materials	46500 @ 930eV	250-1700	waiting for funding.	Phase II project on Dreamline beamline 8m scattering arm	Yong Wang wangyong@sinap.ac.cn
TPS (Taiwan)	Low-energy excitations of transition metal compounds.	42000 @ 900eV	400-1200	Under construction (11/2015)	Dragon type beamline. Energy compensation scheme (AGS-AGM) Polarization analysis. 7.5m long scattering arm	Di-Jing Huang djhuang@nsrrc.org.tw
CLS (Canada)						
SPRING8 (Japan)						

Hard x-ray RIXS beamlines

Facility	Beamline	Energy	Resolution	Analyzer	Spectrometer	Materials	Contact
APS (US)	Sector 27	6~15 keV	25~ 200 meV	Single analyzer	Vertical/ Horizontals cattering	3d and 5d TM and RE, etc	J. Kim
Spring-8 (Japan)	BL 11 XU	6~10 keV	0.1~1 eV	Single analyzer	Horizontal scattering	3d and 5d TM and etc	Kenji Ishii
Spring-8 (Japan)	BL 12 XU	8~32 keV	1 eV	Single analyzer	Horizontal scattering	3d TM	Nozomu Hiraoka
ESRF (France)	ID 20	4~20 keV	25 meV~ 2eV	Five analyzers	Vertical/ Horizontals cattering	3d and 5d TM and etc	Marco Moretti
Desy (Germany)	P 01	5~20 keV	25 meV ~ 1eV	Single analyzer	Vertical/ Horizontals cattering	3d TM	Hasan Yavas
SSRF (China)	Planned						Xuerong Liu

Hard x-ray RIXS @ 1C beamline of PLS-II

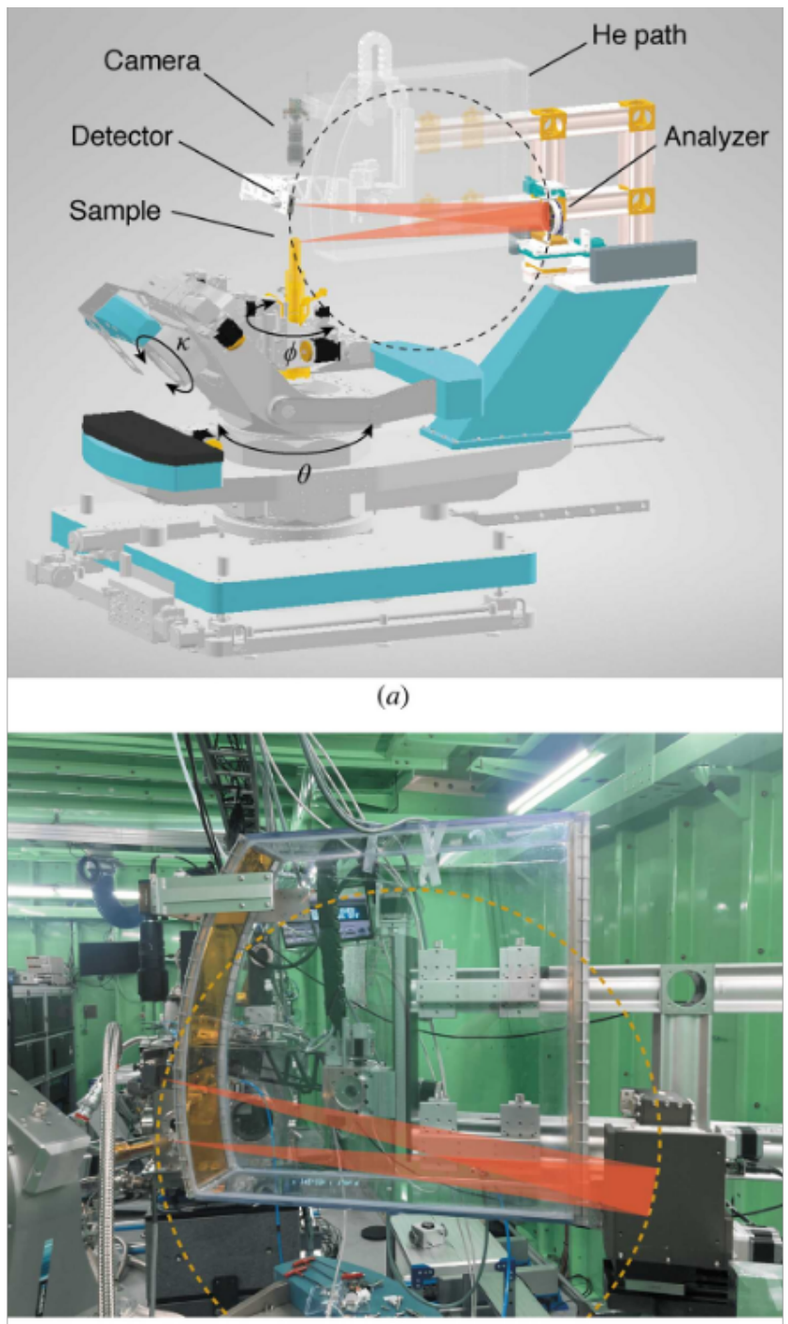

(a)

(b)

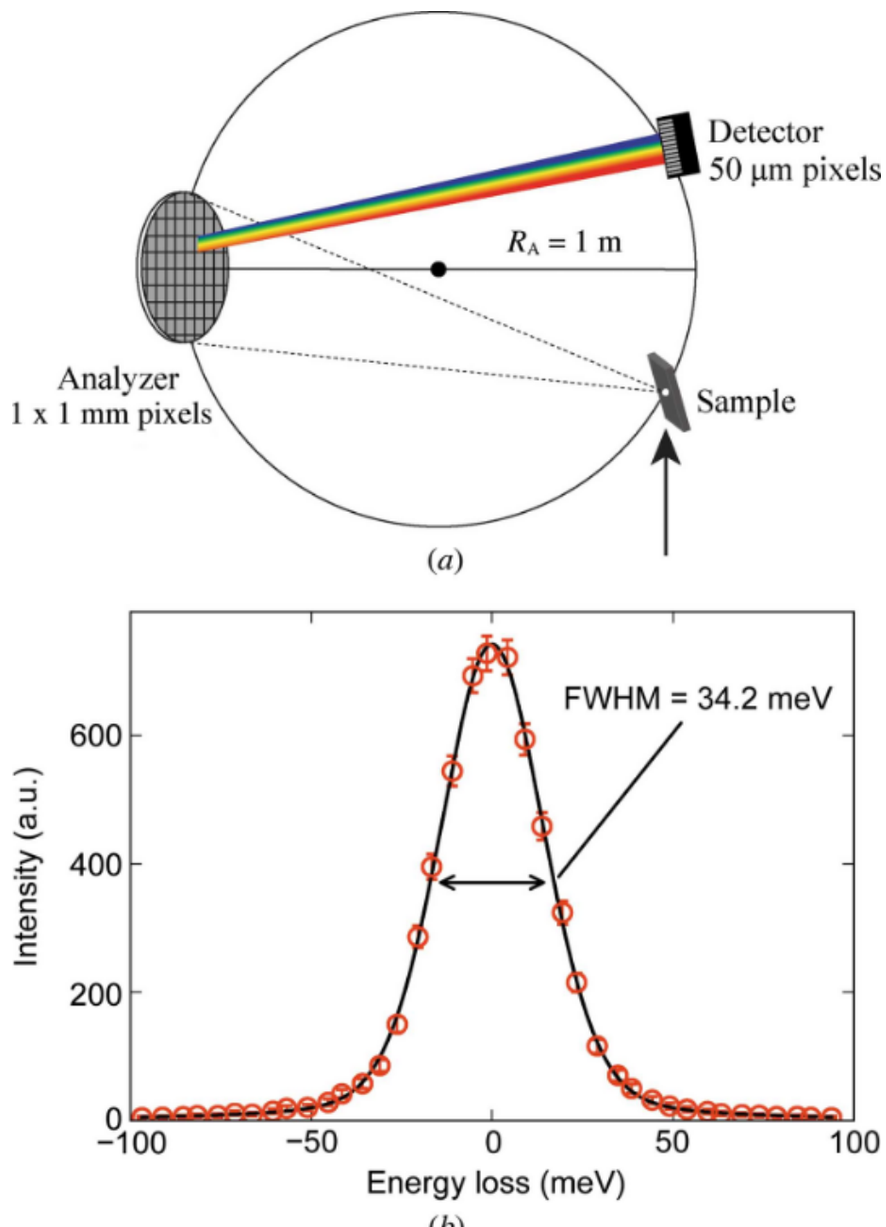

(a)

(b)

JOURNAL OF SYNCHROTRON RADIATION

Kim *et al.*

Volume 30 | **Part 3** | May 2023 | Pages 643–649 | 10.11107/S1600577523001625

Basic Principles

Photon-electron interaction

$$H' = \frac{e^2}{2m_e c^2}\sum_i \boldsymbol{A}(\boldsymbol{r}_i)^2 - \frac{e^2\hbar}{2m_e{}^2 c^4}\sum_i \boldsymbol{s}_i \cdot (\frac{\partial \boldsymbol{A}}{\partial t} \times \boldsymbol{A}) - \frac{e}{m_e c}\sum_i \boldsymbol{A}(\boldsymbol{r}_i)\cdot \boldsymbol{p} - \frac{e^2\hbar}{2m_e{}^2 c^4}\sum_i \boldsymbol{s}_i \cdot (\nabla \times \boldsymbol{A}(\boldsymbol{r}_i))$$

$$\begin{aligned}
\langle \phi_n | e^{-i\vec{k}\cdot\vec{r}}\hat{\epsilon}\cdot\vec{p}_e|\phi_i\rangle &\approx \hat{\epsilon}\cdot\langle\phi_n|\vec{p}_e|\phi_i\rangle \\
&= \frac{im}{\hbar}\hat{\epsilon}\cdot\langle\phi_n|[H,\vec{r}]|\phi_i\rangle \\
&= \frac{im}{\hbar}(E_n - E_i)\hat{\epsilon}\cdot\langle\phi_n|\vec{r}|\phi_i\rangle \\
&= \frac{im(E_n - E_i)}{\hbar}\langle\phi_n|\hat{\epsilon}\cdot\vec{r}|\phi_i\rangle
\end{aligned}$$

Quadrupole transition (E2)

ΔL=2

$$e^{-i\vec{k}\cdot\vec{r}} \approx 1 - i\vec{k}\cdot\vec{r} + \ldots$$

ΔL=1

Dipole transition (E1)

X-ray absorption intensity

$$I \propto |\langle \phi_n | \vec{\varepsilon}\cdot\vec{r}|\phi_i\rangle|^2$$

Resonance scattering

Second-order process

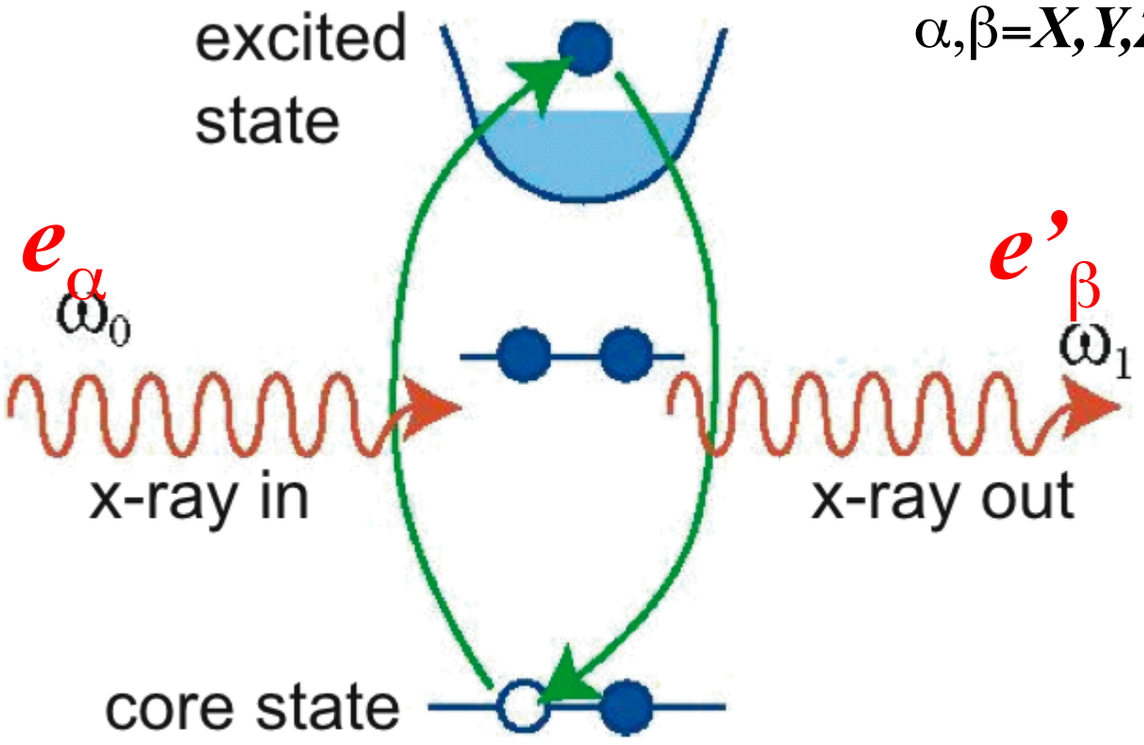

$\alpha,\beta = X, Y, Z$

$$I \propto \left| \frac{\langle \phi_f | \vec{\varepsilon}^* \cdot \vec{r} | \phi_n \rangle \langle \phi_n | \vec{\varepsilon} \cdot \vec{r} | \phi_i \rangle}{\omega - E_n + E_i + i\Gamma/2} \right|^2$$

ray absorption + X ray emission in one coherent quantum process.

What does RIXS measure?

Correlation functions

Experiments measure correlation functions

Ex: Neutron and x-ray measure spin and density correlation functions, respectively.

$$S_s(q,\omega) = \int drdt \langle S^+(r,t)S^-(0,0)\rangle \quad S_\rho(q,\omega) = \int drdt \langle \rho(r,t)\rho(0,0)\rangle$$

$$S_s(q,\omega) = \sum_f |\langle f|S|i\rangle|^2 \delta(E_i - E_f + \hbar\omega)$$

RIXS process

$$\frac{\delta^2\sigma}{\delta\Omega\delta\omega} \propto \lim_{\Gamma\to 0+} \sum_f \left| \langle f | T^{\dagger}_{\varepsilon_o} \frac{1}{\omega_i + E_i + i\Gamma/2 - H} T_{\varepsilon_i} |i\rangle \right|^2 \delta(\omega_i - \omega_o + E_i - E_f)$$

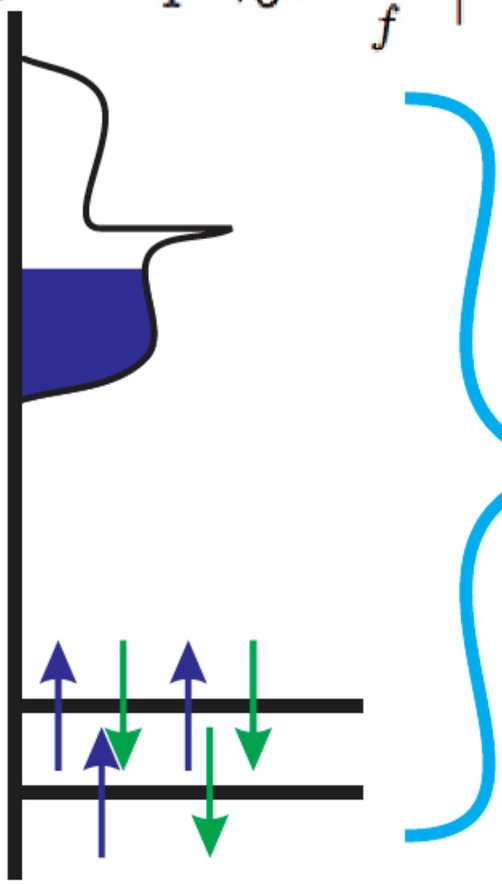

courtesy of M. Haverkort

RIXS process

$$\frac{\delta^2\sigma}{\delta\Omega\delta\omega} \propto \lim_{\Gamma\to 0+} \sum_f \left| \langle f | T^{\dagger}_{\varepsilon_o} \frac{1}{\omega_i + E_i + i\Gamma/2 - H} T_{\varepsilon_i} | i \rangle \right|^2 \delta(\omega_i - \omega_o + E_i - E_f)$$

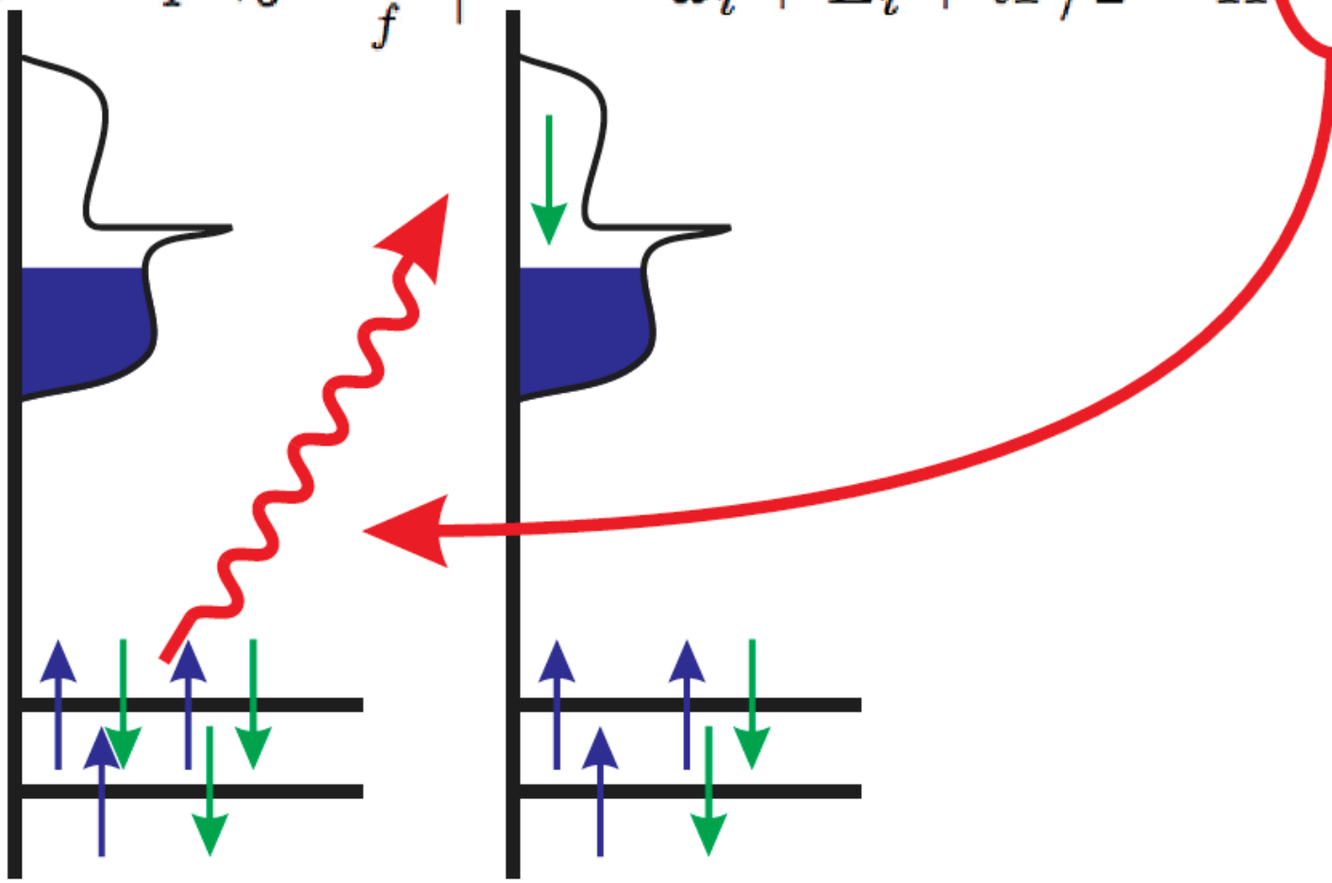

courtesy of M. Haverkort

RIXS process

$$\frac{\delta^2\sigma}{\delta\Omega\delta\omega} \propto \lim_{\Gamma\to 0+} \sum_f \left| \langle f | T^{\dagger}_{\varepsilon_o} \frac{1}{\omega_i + E_i + i\Gamma/2 - H} T_{\varepsilon_i} | i \rangle \right|^2 \delta(\omega_i - \omega_o + E_i - E_f)$$

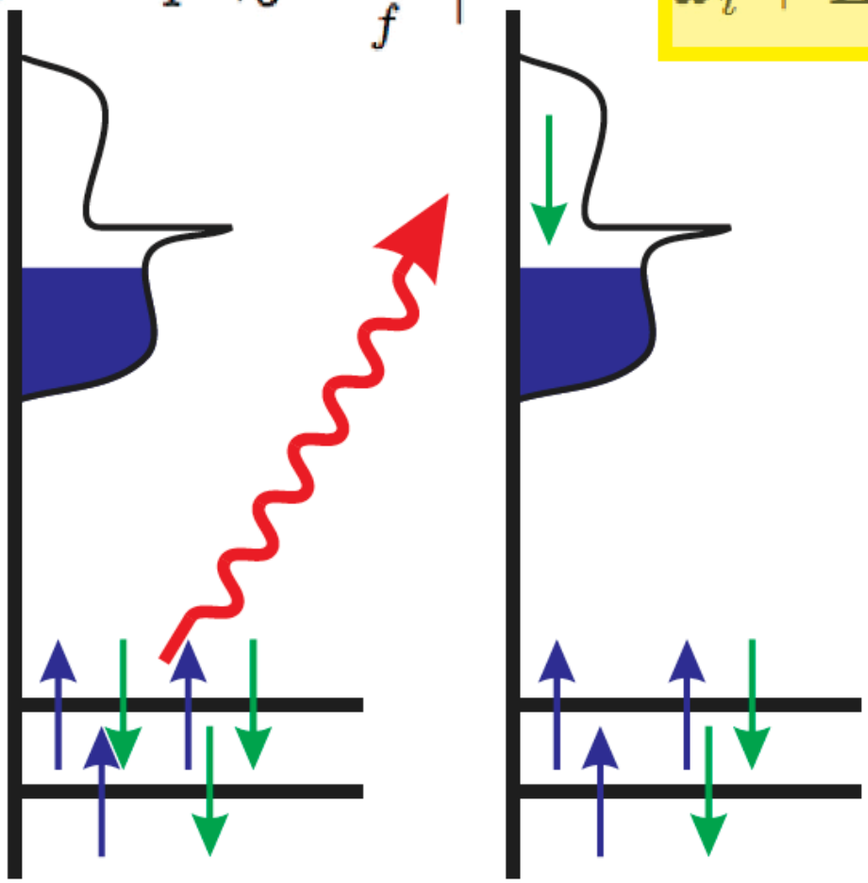

courtesy of M. Haverkort

RIXS process

$$\frac{\delta^2\sigma}{\delta\Omega\delta\omega} \propto \lim_{\Gamma\to 0+} \sum_f \left| \langle f | T^{\dagger}_{\varepsilon_o} \frac{1}{\omega_i + E_i + i\Gamma/2 - H} T_{\varepsilon_i} | i \rangle \right|^2 \delta(\omega_i - \omega_o + E_i - E_f)$$

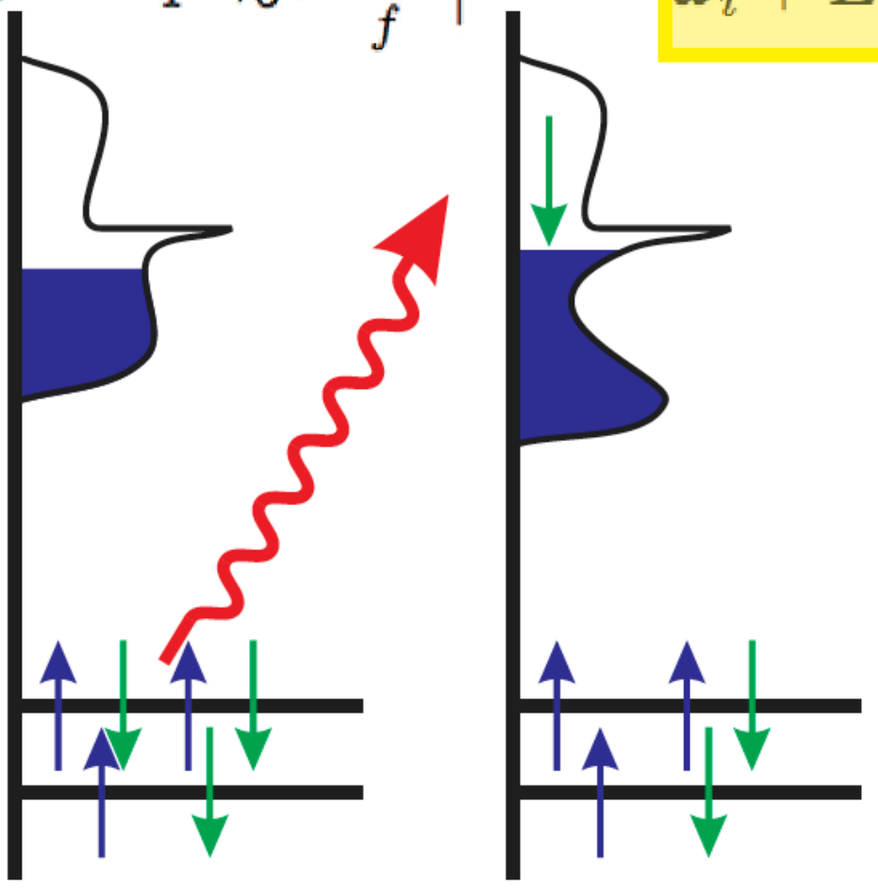

courtesy of M. Haverkort

RIXS process

$$\frac{\delta^2\sigma}{\delta\Omega\delta\omega} \propto \lim_{\Gamma\to 0+} \sum_f \left| \langle f | T^{\dagger}_{\varepsilon_o} \frac{1}{\omega_i + E_i + i\Gamma/2 - H} T_{\varepsilon_i} | i \rangle \right|^2 \delta(\omega_i - \omega_o + E_i - E_f)$$

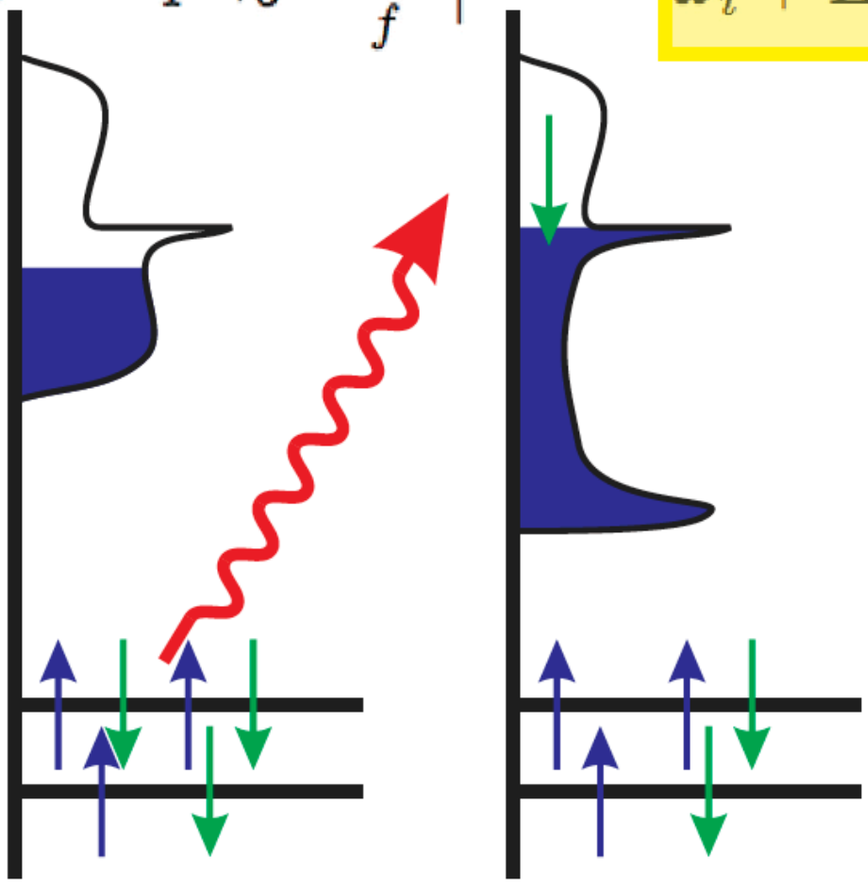

courtesy of M. Haverkort

RIXS process

$$\frac{\delta^2\sigma}{\delta\Omega\delta\omega} \propto \lim_{\Gamma\to 0+} \sum_f \left| \langle f | T^{\dagger}_{\varepsilon_o} \frac{1}{\omega_i + E_i + i\Gamma/2 - H} T_{\varepsilon_i} | i \rangle \right|^2 \delta(\omega_i - \omega_o + E_i - E_f)$$

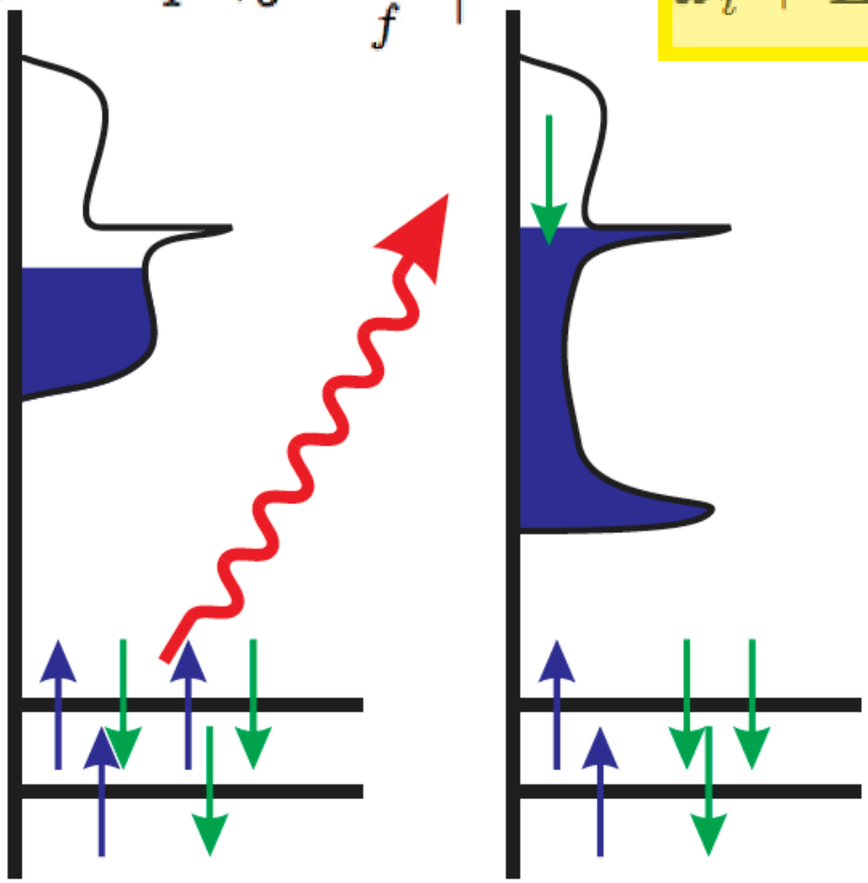

courtesy of M. Haverkort

RIXS process

$$\frac{\delta^2\sigma}{\delta\Omega\delta\omega} \propto \lim_{\Gamma\to 0+} \sum_f \left| \langle f | T^{\dagger}_{\varepsilon_o} \frac{1}{\omega_i + E_i + i\Gamma/2 - H} T_{\varepsilon_i} | i \rangle \right|^2 \delta(\omega_i - \omega_o + E_i - E_f)$$

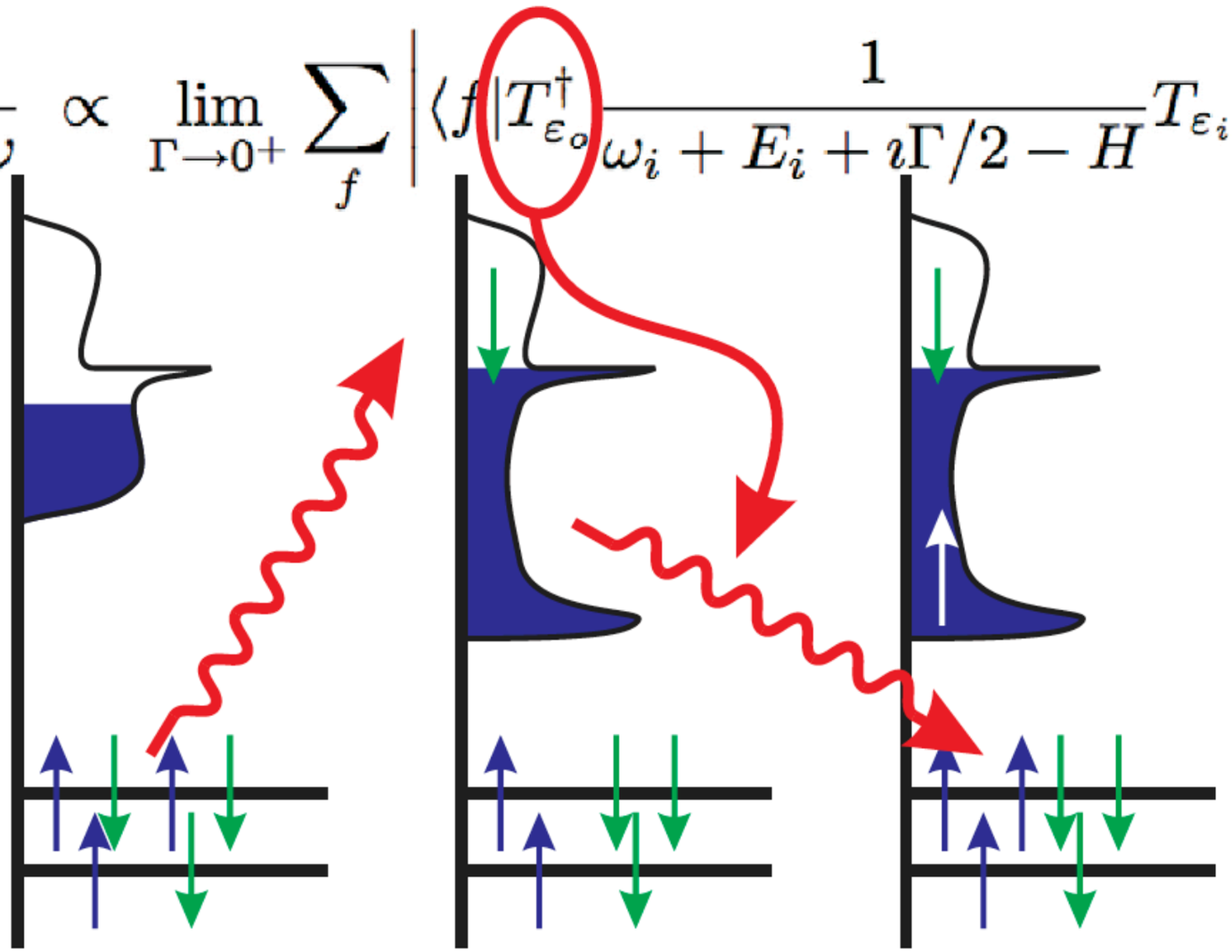

courtesy of M. Haverkort

RIXS process

$$\frac{\delta^2\sigma}{\delta\Omega\delta\omega} \propto \lim_{\Gamma\to 0^+} \sum_f \left| \langle f | T^\dagger_{\epsilon_o} \frac{1}{\omega_i + E_i + i\Gamma/2 - H} T_{\epsilon_i} |i\rangle \right|^2 \delta(\omega_i - \omega_o + E_i - E_f)$$

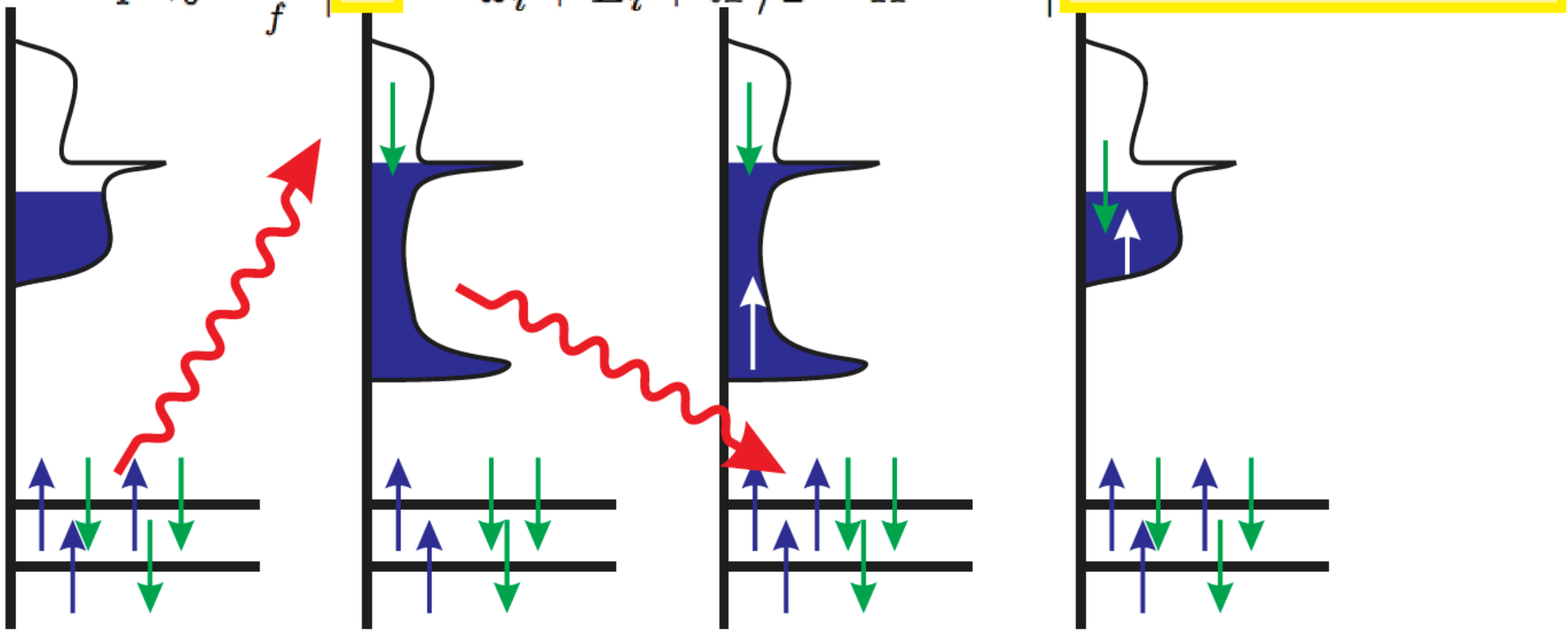

courtesy of M. Haverkort

RIXS process

$$\frac{\delta^2\sigma}{\delta\Omega\delta\omega} \propto \lim_{\Gamma\to 0+}\sum_f \left|\langle f|T^\dagger_{\varepsilon_o}\frac{1}{\omega_i+E_i+i\Gamma/2-H}T_{\varepsilon_i}|i\rangle\right|^2 \delta(\omega_i-\omega_o+E_i-E_f)$$

$$R^{\varepsilon_i\varepsilon_o}_{\omega_i}$$

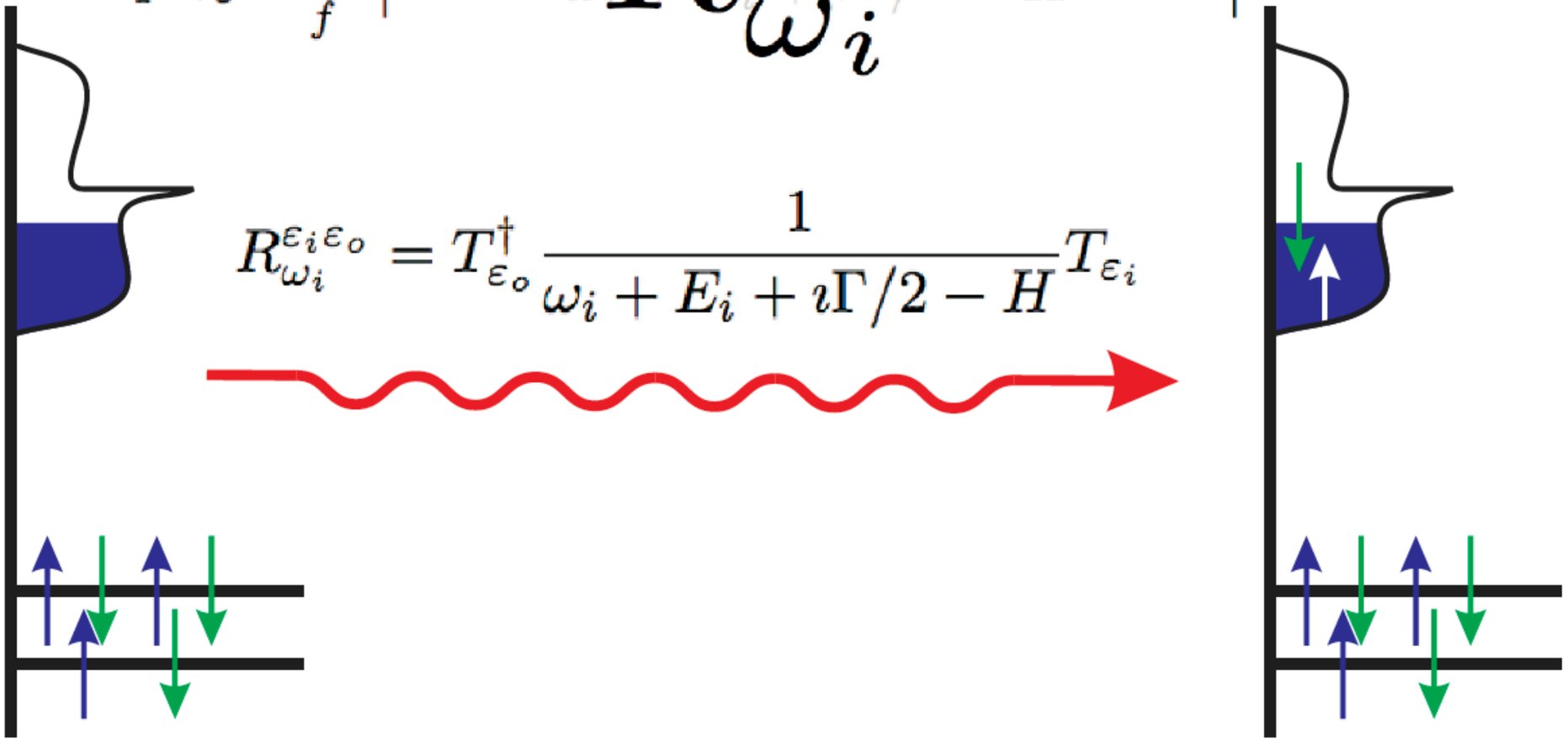

$$R^{\varepsilon_i\varepsilon_o}_{\omega_i} = T^\dagger_{\varepsilon_o}\frac{1}{\omega_i+E_i+i\Gamma/2-H}T_{\varepsilon_i}$$

antisymmetric	$(\epsilon_\alpha\epsilon'_\beta-\epsilon_\beta\epsilon'_\alpha)$	dipole
symmetric	$(\epsilon_\alpha\epsilon'_\beta+\epsilon_\beta\epsilon'_\alpha)$	quadrupole

courtesy of M. Haverkort

RIXS operators for t_{2g} orbital systems

unquenched orbital angular momentum

"fast collision approximation"

$$R_{\omega_i}^{\varepsilon_i \varepsilon_o} = T_{\varepsilon_o}^{\dagger} \frac{1}{\omega_i + E_i + i\Gamma/2 - H} T_{\varepsilon_i}$$

c number

$$R \propto D^{\dagger} D = \tfrac{1}{3}(R_Q + i R_M)$$

$$R_Q = \sum_{\alpha} \epsilon_\alpha \epsilon'_\alpha Q_{\alpha\alpha} - \frac{1}{2} \sum_{\alpha > \beta} (\epsilon_\alpha \epsilon'_\beta + \epsilon_\beta \epsilon'_\alpha) Q_{\alpha\beta}$$

$$R_M = \tfrac{1}{2}(\boldsymbol{\epsilon} \times \boldsymbol{\epsilon}') \cdot \mathbf{N}.$$

Q_{zz} (quadrupole)	L_3 edge	L_2 edge
$d^1, (-1)d^5$	$-2L_z^2 + 2L_z S_z$	$-L_z^2 - 2L_z S_z$
$d^2, (-1)d^4$	$2L_z^2 + L_z S_z$	$L_z^2 - L_z S_z$
Q_{xy} (quadrupole)	L_3 edge	L_2 edge
$d^1, (-1)d^5$	$-2L_x L_y - 2L_y L_x + 2L_x S_y + 2L_y S_x$	$-L_x L_y - L_y L_x - 2L_x S_y - 2L_y S_x$
$d^2, (-1)d^4$	$2L_x L_y + 2L_y L_x + L_x S_y + L_y S_x$	$L_x L_y + L_y L_x - L_x S_y - L_y S_x$
N_z (magnetic)	L_3 edge	L_2 edge
d^1, d^5	$2L_z - 4S_z + 8L_z^2 S_z - 2L_z(\mathbf{L}\cdot\mathbf{S}) - 2(\mathbf{L}\cdot\mathbf{S})L_z$	$L_z + 4S_z - 8L_z^2 S_z + 2L_z(\mathbf{L}\cdot\mathbf{S}) + 2(\mathbf{L}\cdot\mathbf{S})L_z$
d^2, d^4	$2L_z - 4L_z^2 S_z + L_z(\mathbf{L}\cdot\mathbf{S}) + (\mathbf{L}\cdot\mathbf{S})L_z$	$L_z + 4L_z^2 S_z - L_z(\mathbf{L}\cdot\mathbf{S}) - (\mathbf{L}\cdot\mathbf{S})L_z$
d^3	$(4/3)S_z$	$-(4/3)S_z$

BJK & G. Khaliullin PRB (2017)

Elementary excitations in solids

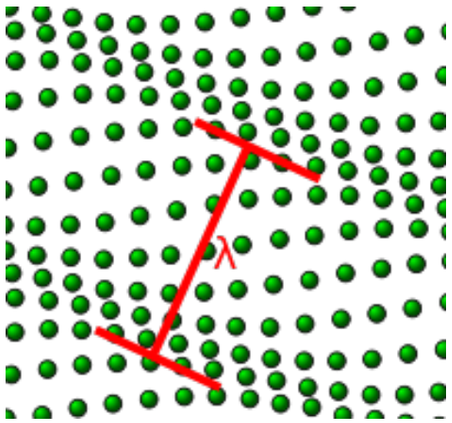

phonon

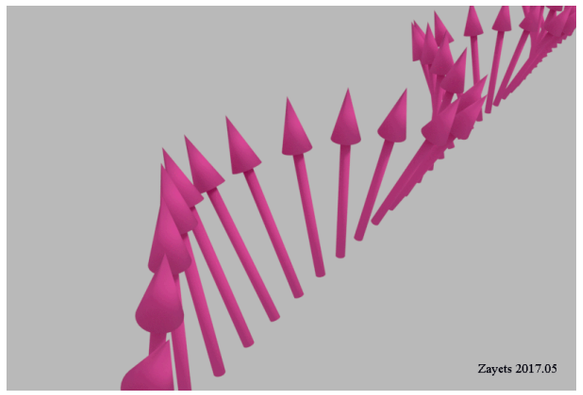

magnon

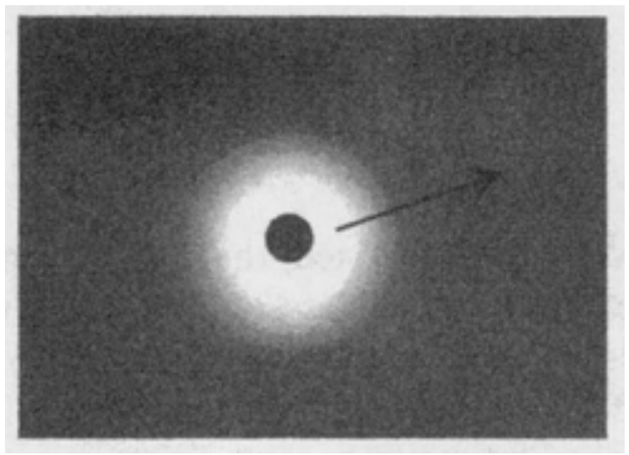

quasi-electron

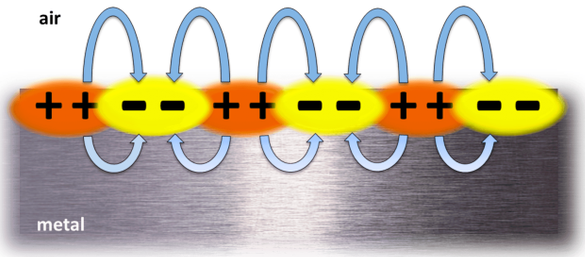

plasmon

And more exotic particles..

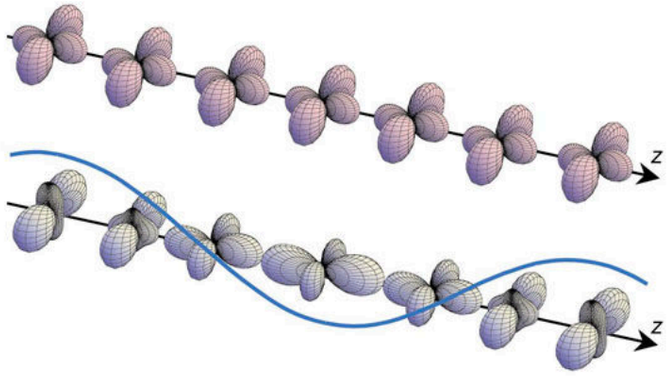

orbiton

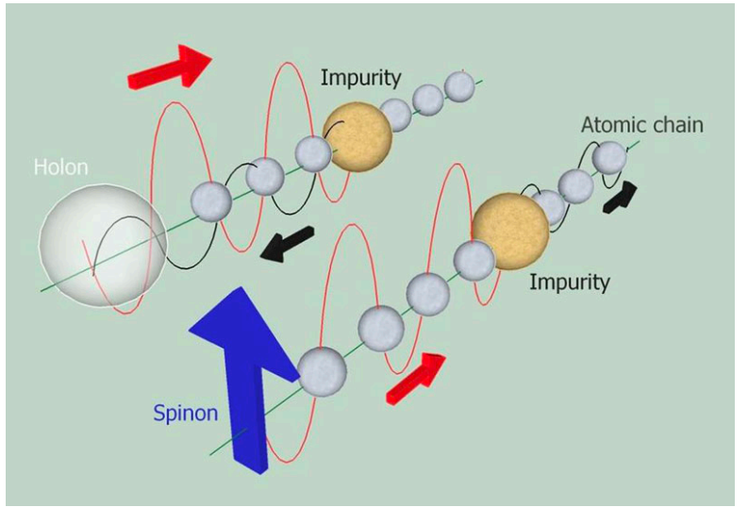

Spinon and holon

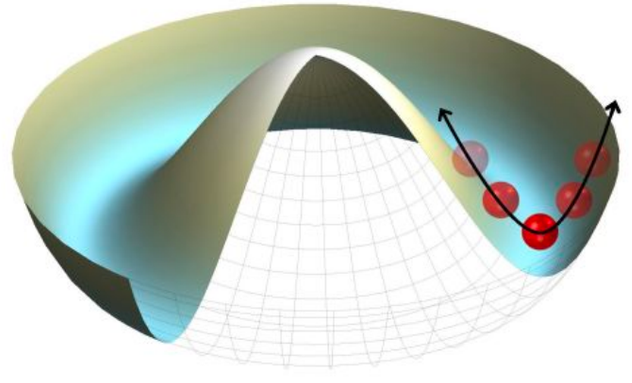

Higgs mode

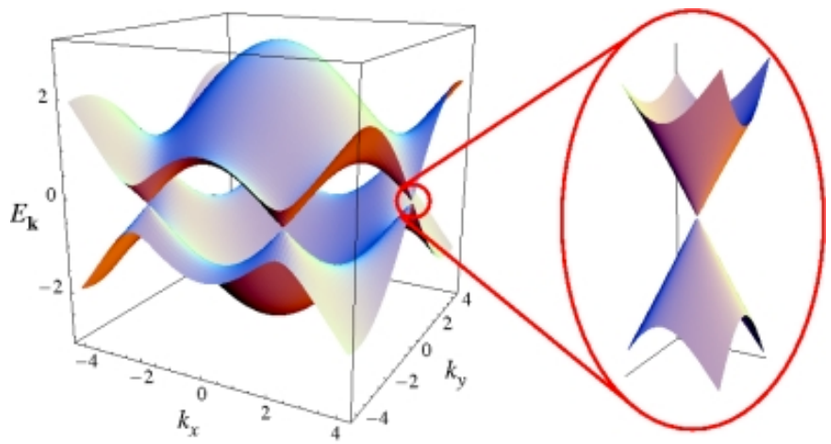

Dirac fermion

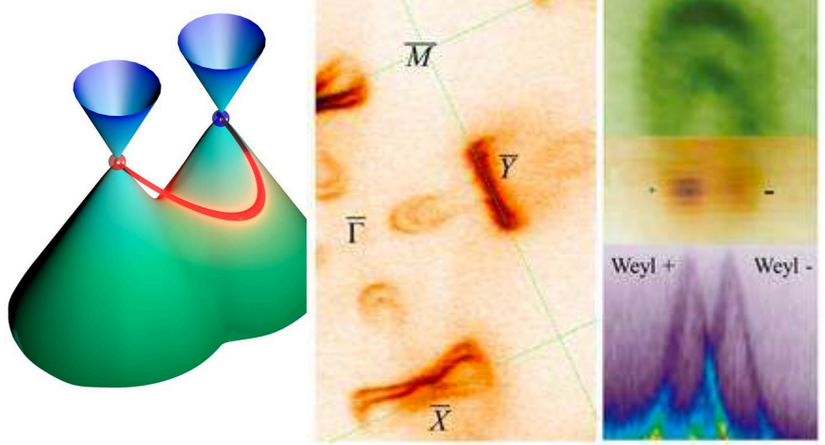

Weyl fermion

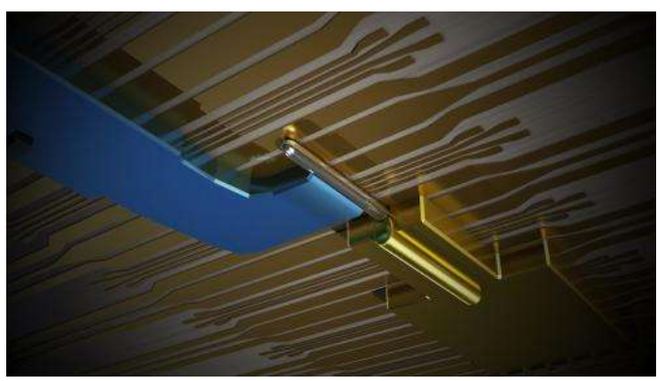

Majonara fermion

Spin waves (or magnons)

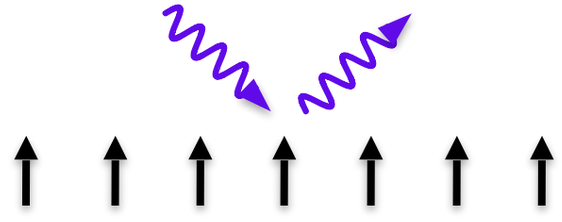

Spin waves (or magnons)

Heisenberg magnet:

$$H = S_z^i S_z^j + S_x^i S_x^j + S_y^i S_y^j$$

$$= S_z^i S_z^j + \frac{1}{2}(S_+^i S_-^j + S_-^i S_+^j)$$

Spin waves (or magnons)

Spin waves (or magnons)

Spin waves (or magnons)

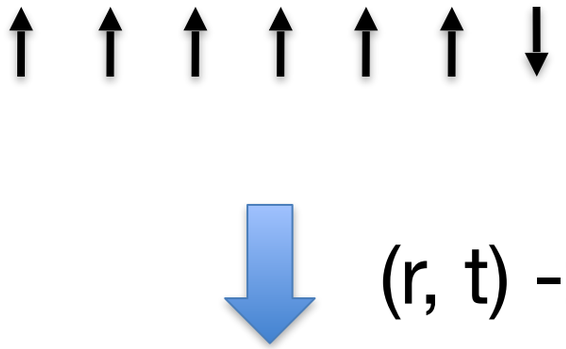

(r, t) -> (q,ω)

dynamic structure factor S(q,ω)

Magnetic excitations in Sr_2IrO_4

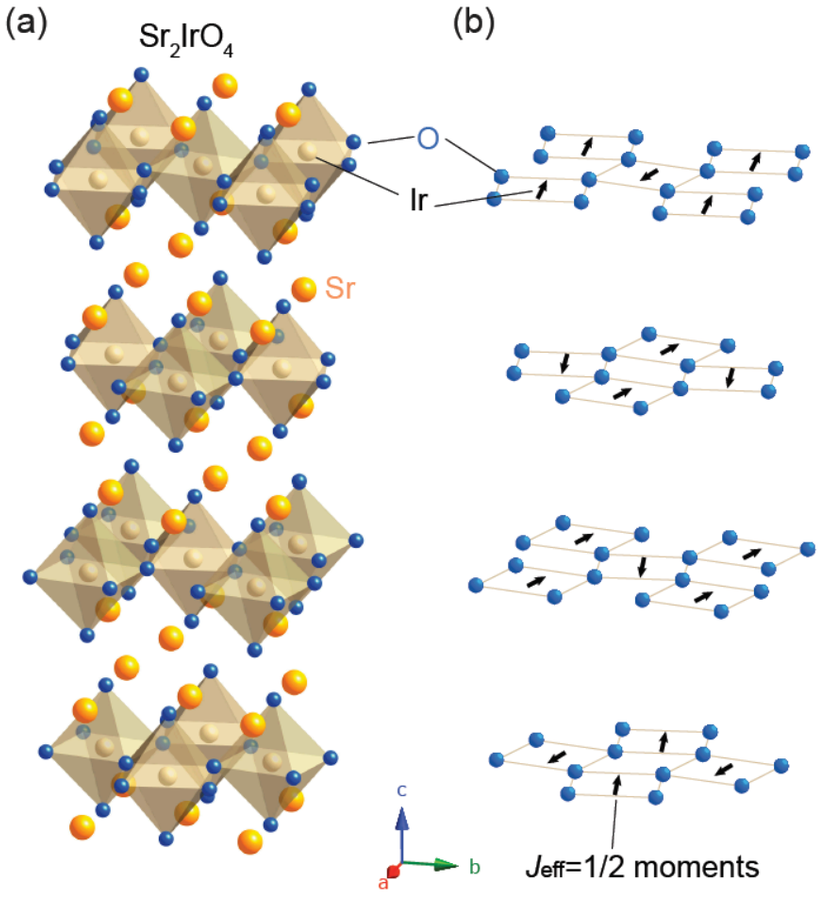

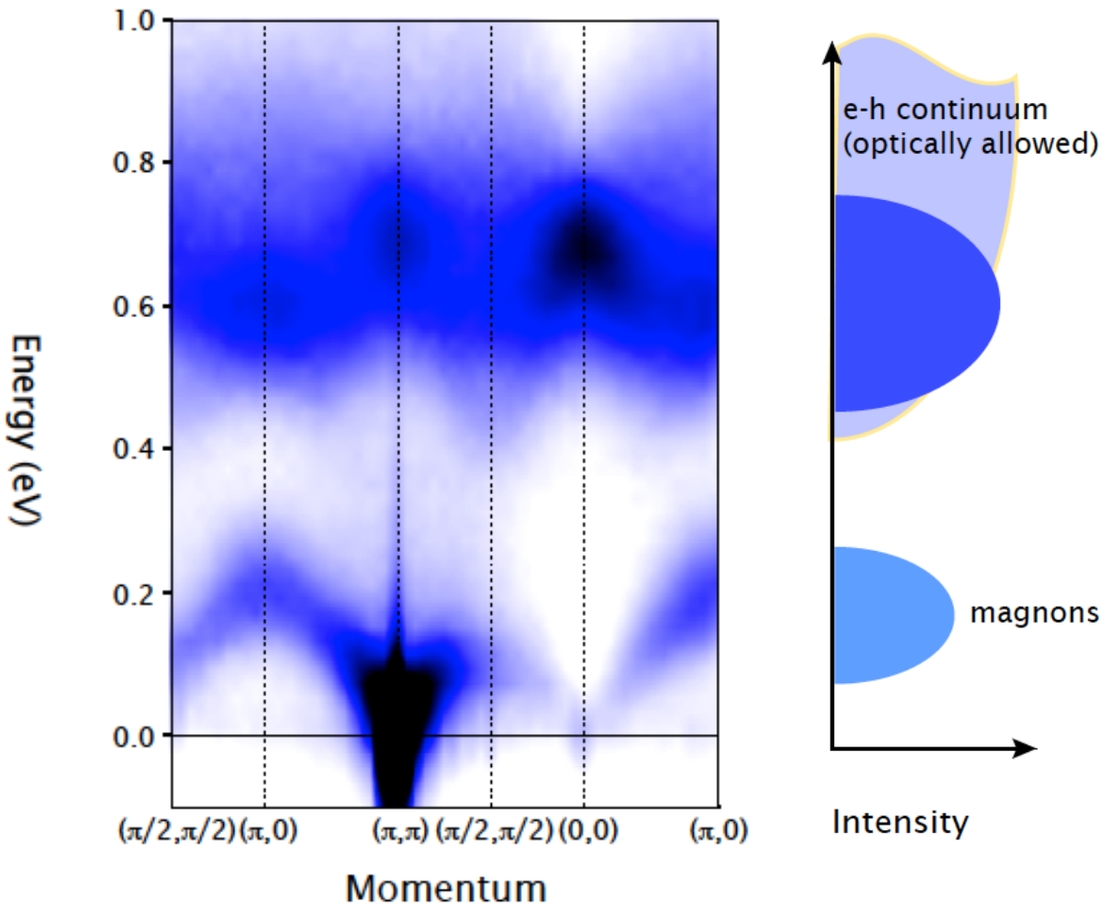

J. Kim & BJK et al. PRL (2012)

Fit to Heisenberg model

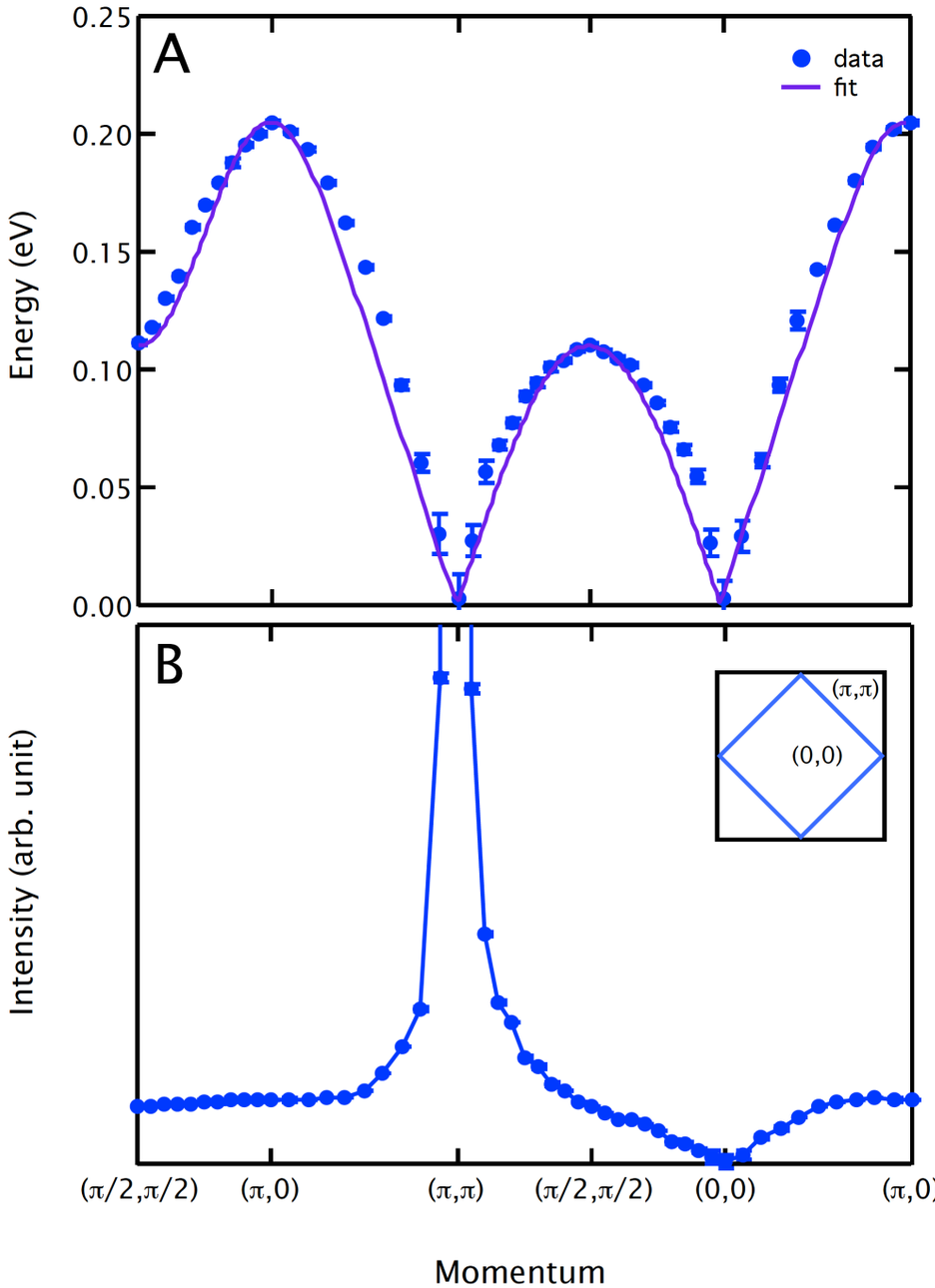

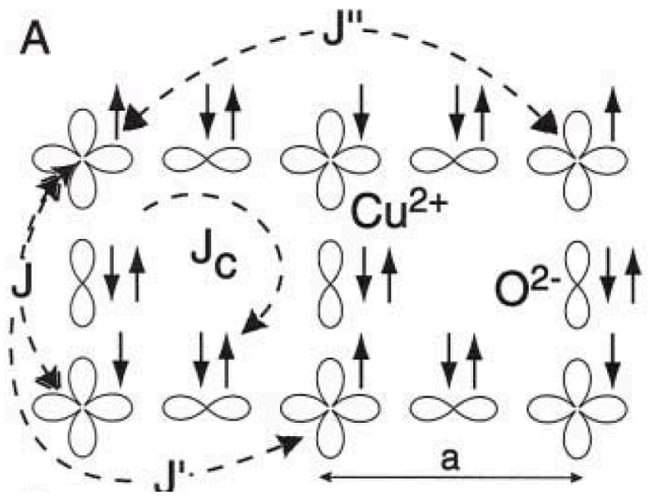

J=60

J′=-20

J″=15

J_c=0 (suppressed)

RIXS vs. Neutron

RIXS data on Sr_2IrO_4

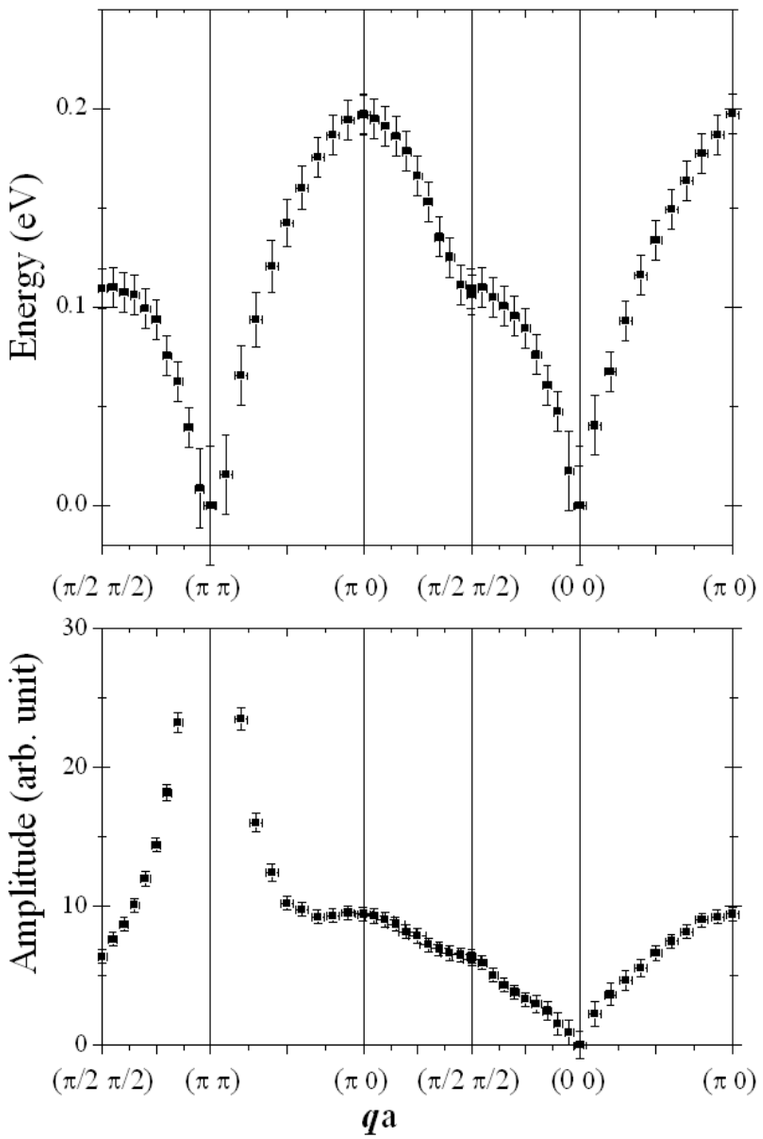

Neutron data on La_2CuO_4

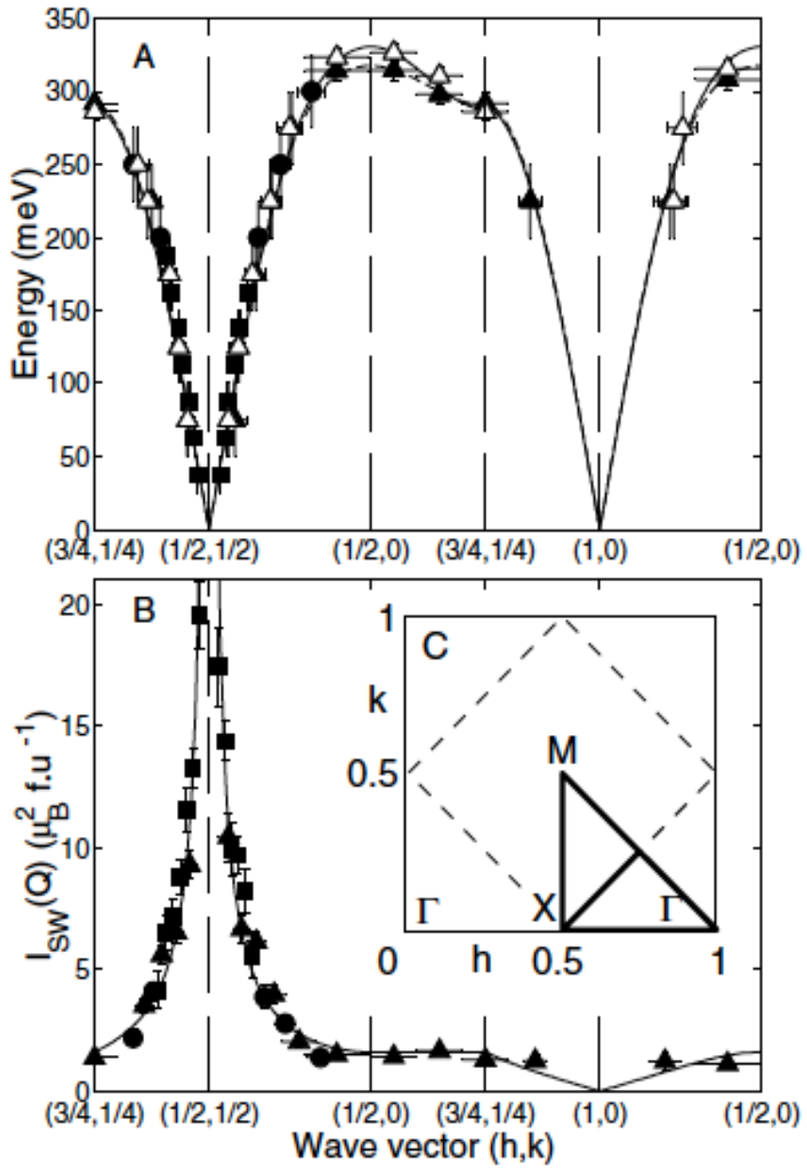

Coldea et al., PRL (2001)

Spin-orbit exciton

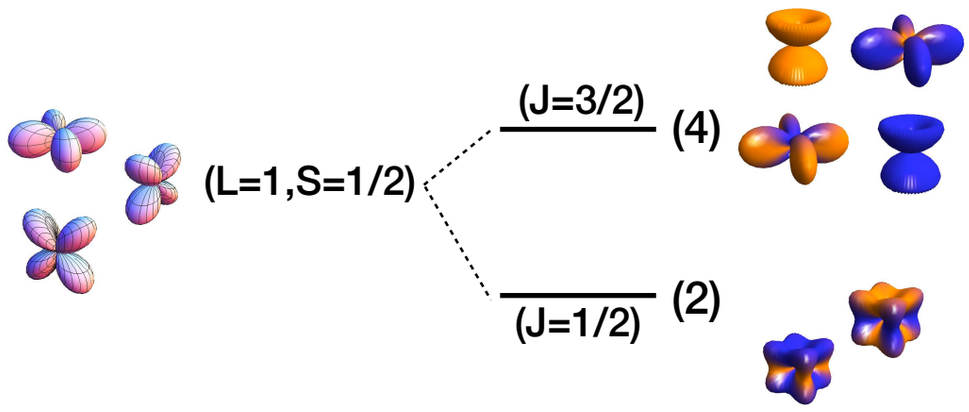

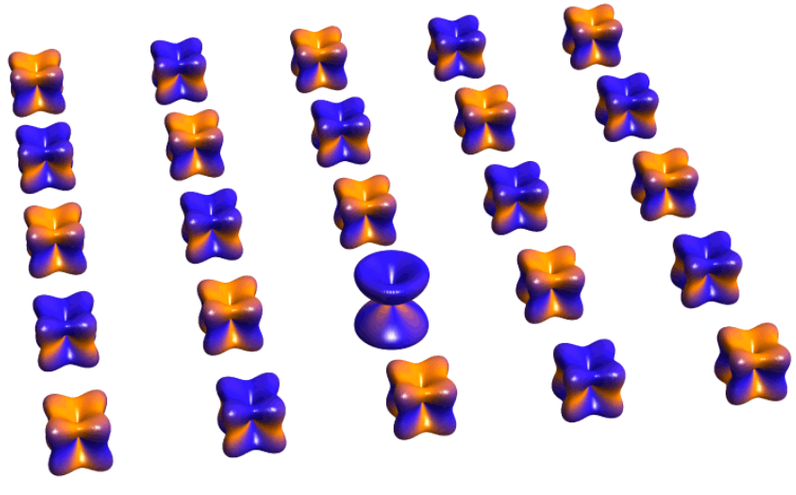

Magnetic excitations in Sr_2IrO_4

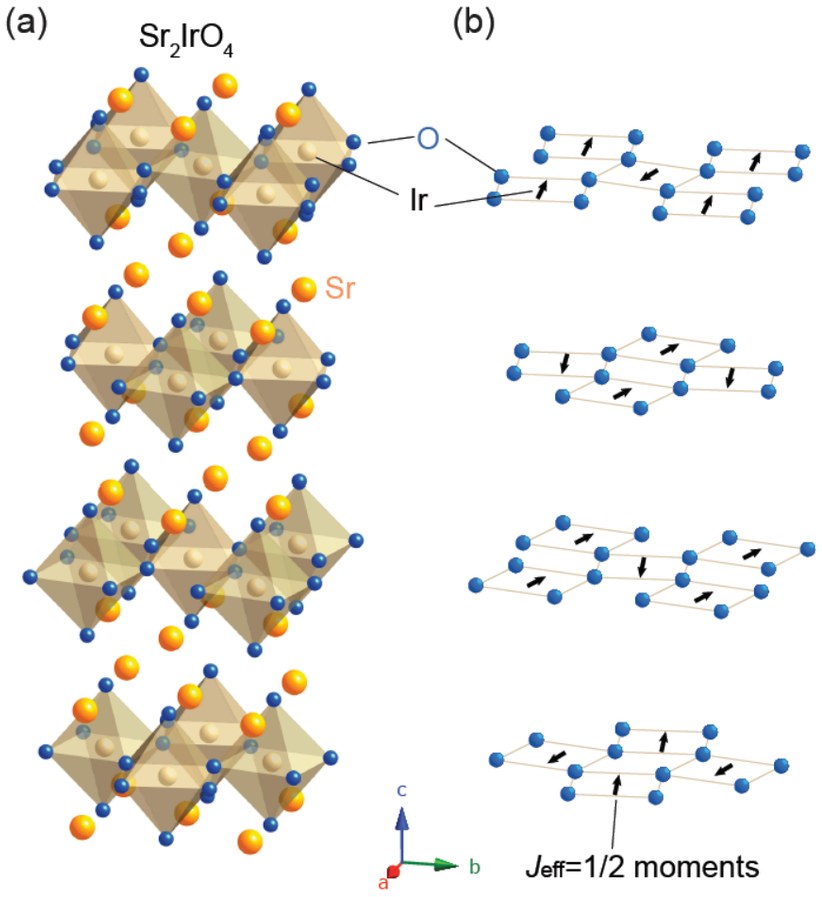

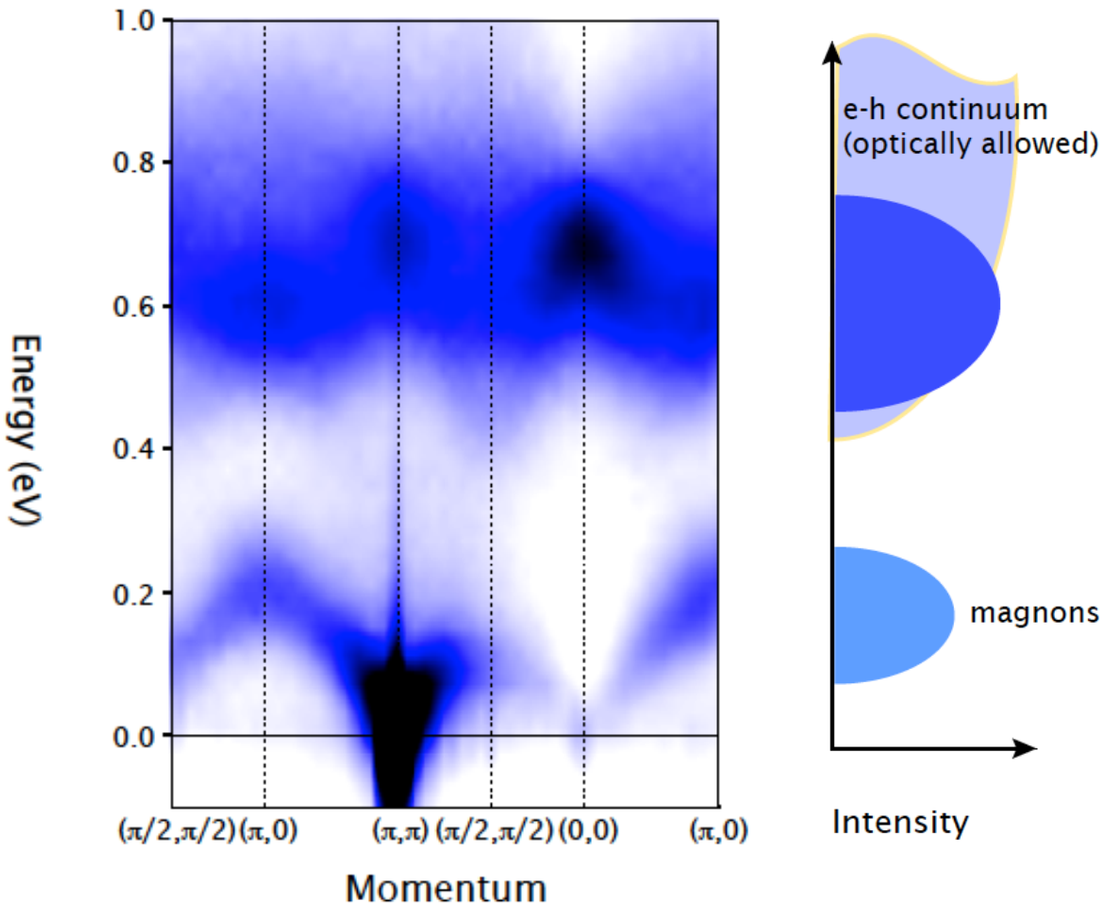

J. Kim & BJK et al. PRL (2012)

Spin-orbital waves

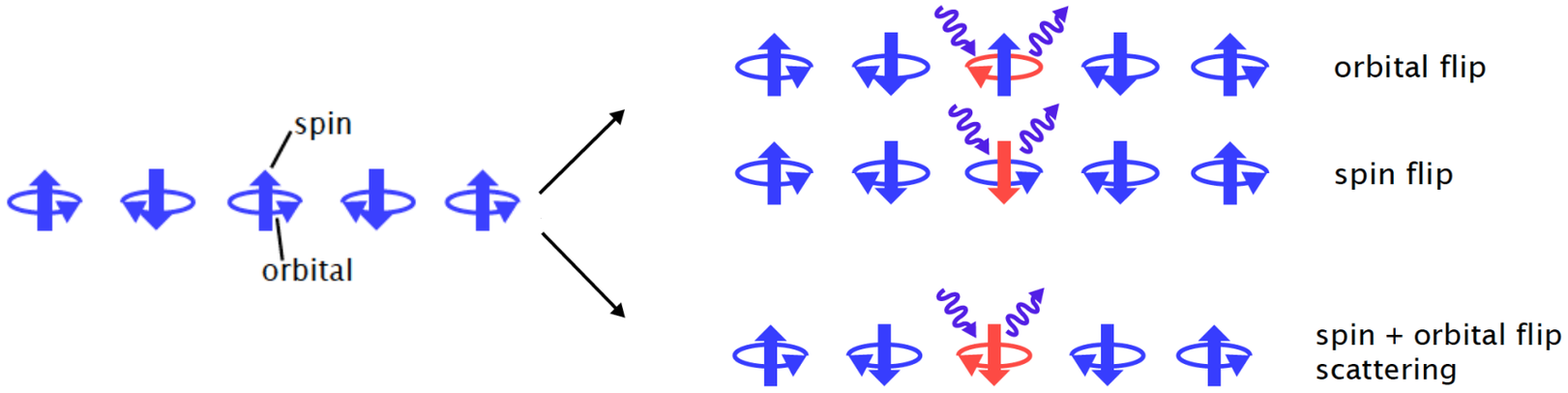

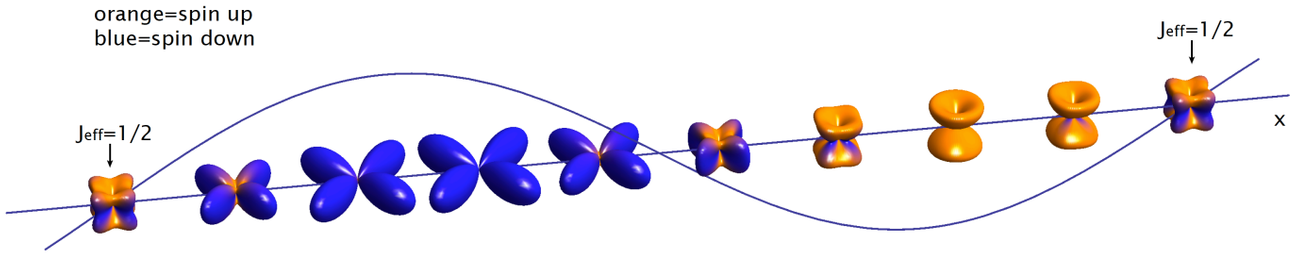

"Orbiton"

E. Saitoh et al., Nature (2001)

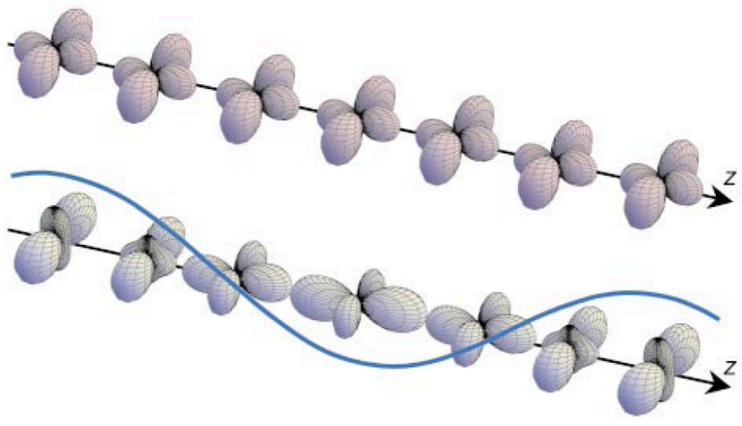

One-hole propagation

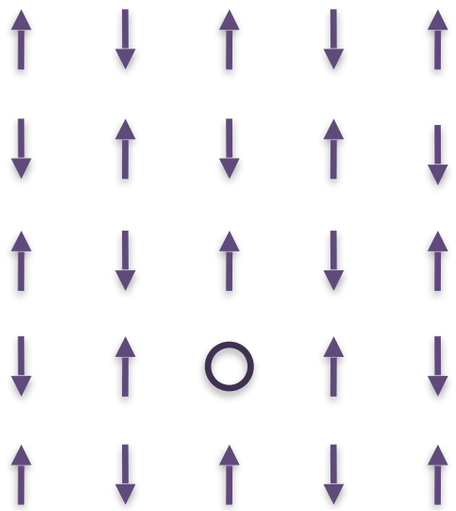

One-hole propagation

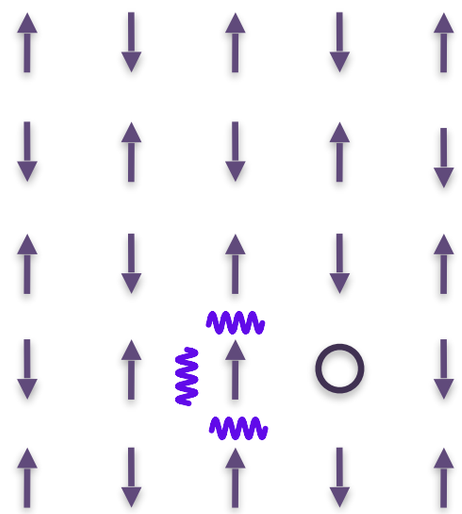

One-hole propagation

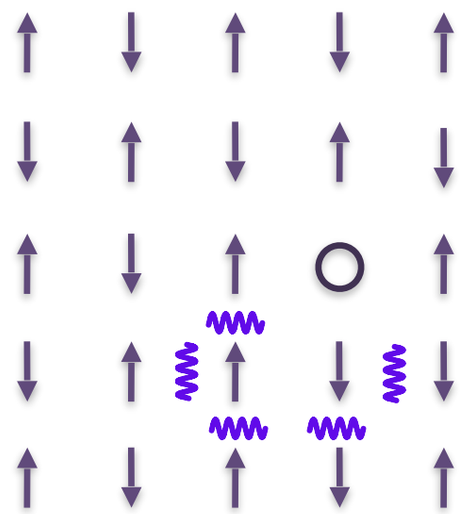

One-hole propagation

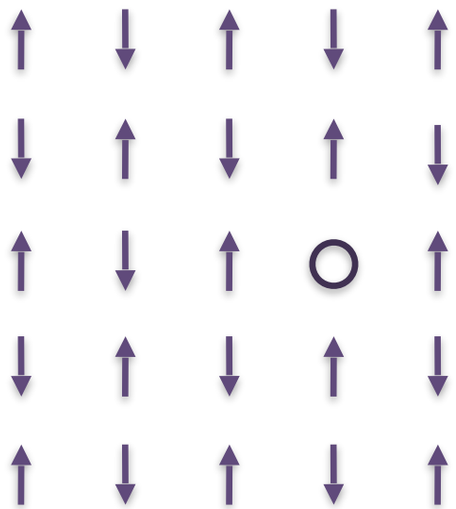

One-hole propagation

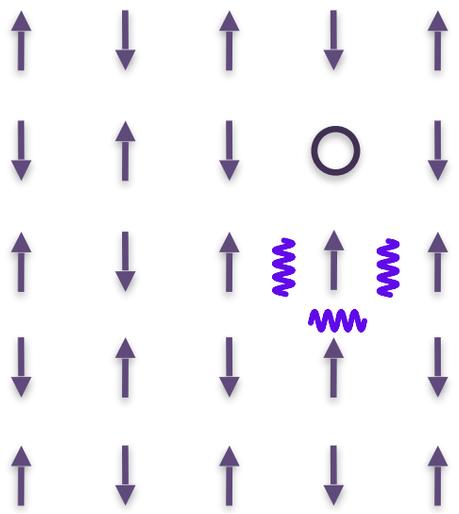

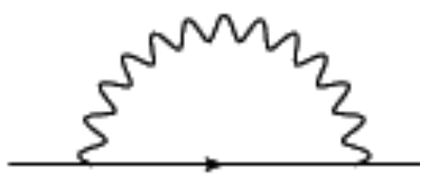

One-hole propagation

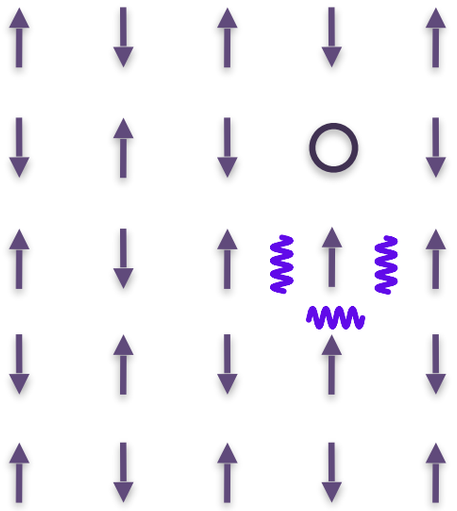

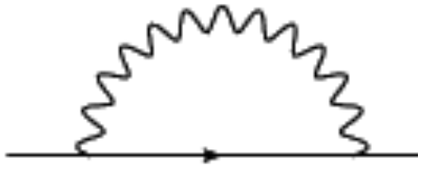

theory (t-J model)

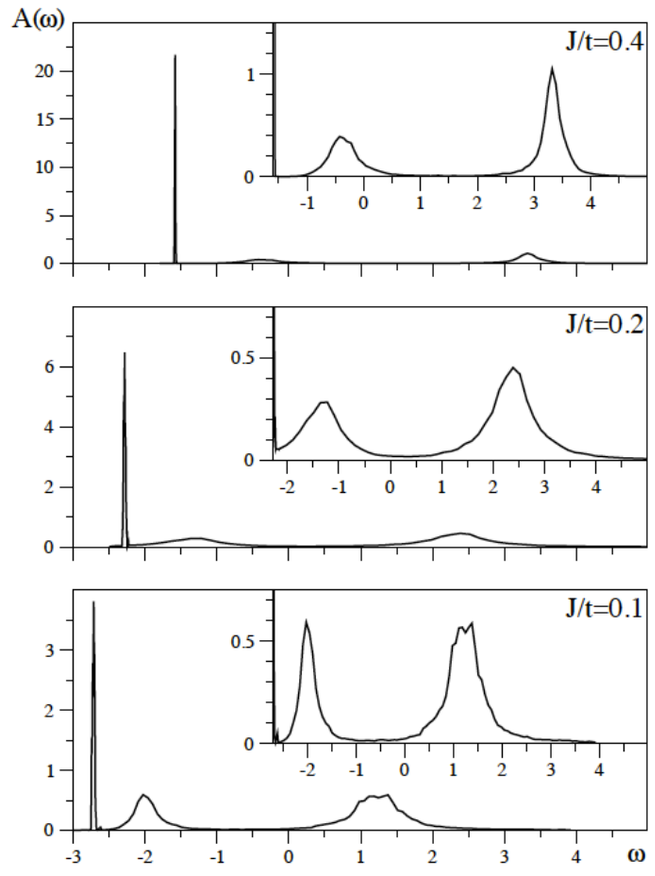

A. S. Mischenko et al. (2001)

ARPES

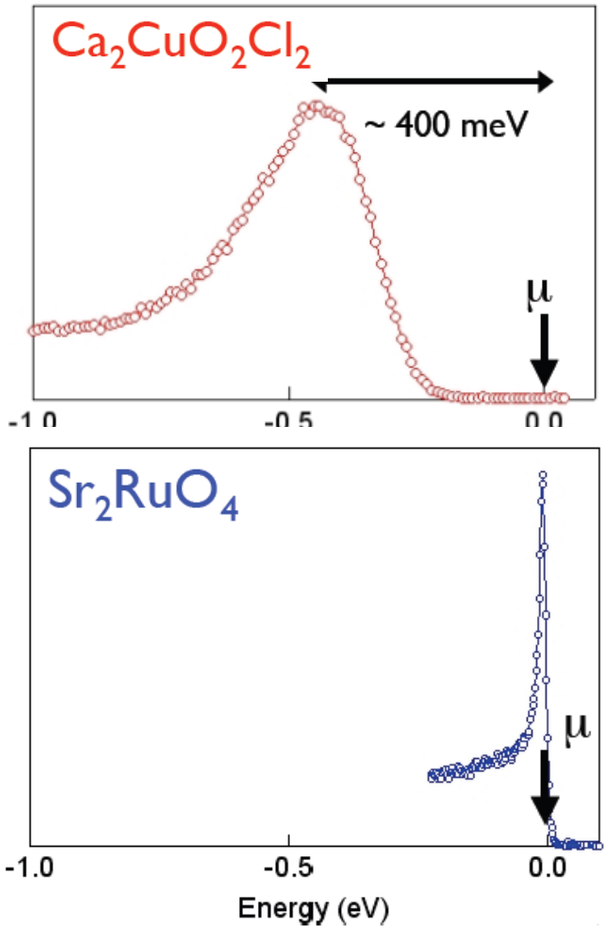

Shen group

One-hole propagation

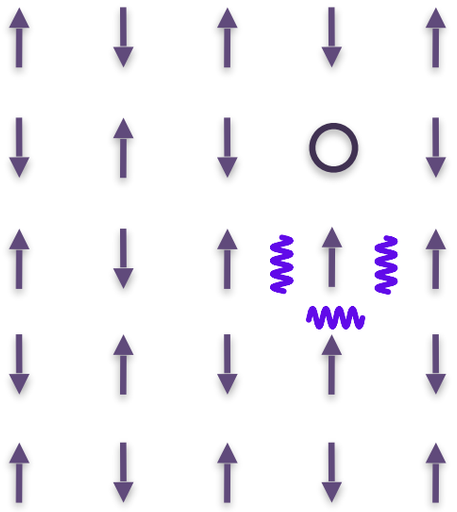

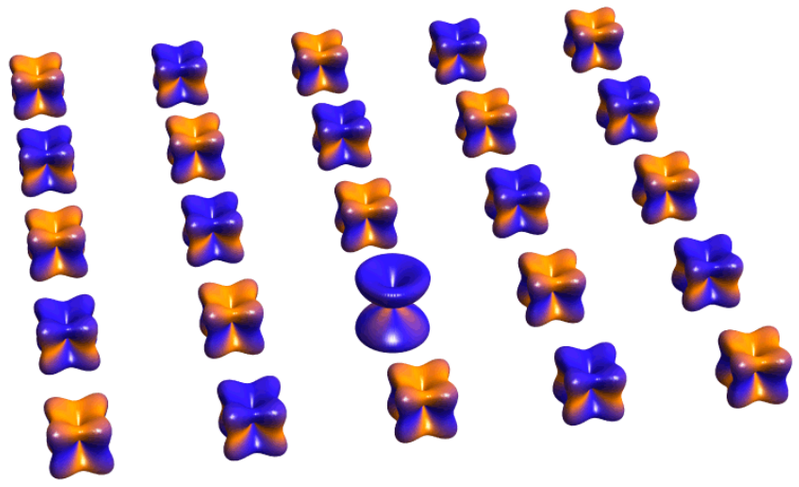

charge e-, spin-1/2 fermion

charge neutral, hard-core boson

One-hole propagation

ARPES

one-hole propagation in $Sr_2CuO_2Cl_2$

B. O. Wells et al., PRL (1995)

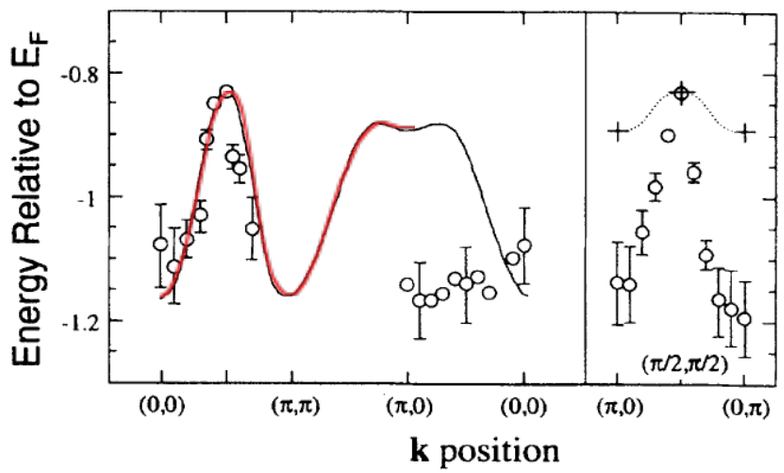

Schmitt-Rink, Varma, Ruckenstein, Phys. Rev. Lett. (1993)
Lee, Nagaosa & Wen, Rev. Mod. Phys. (2006)

RIXS

one-exciton propagation in Sr_2IrO_4

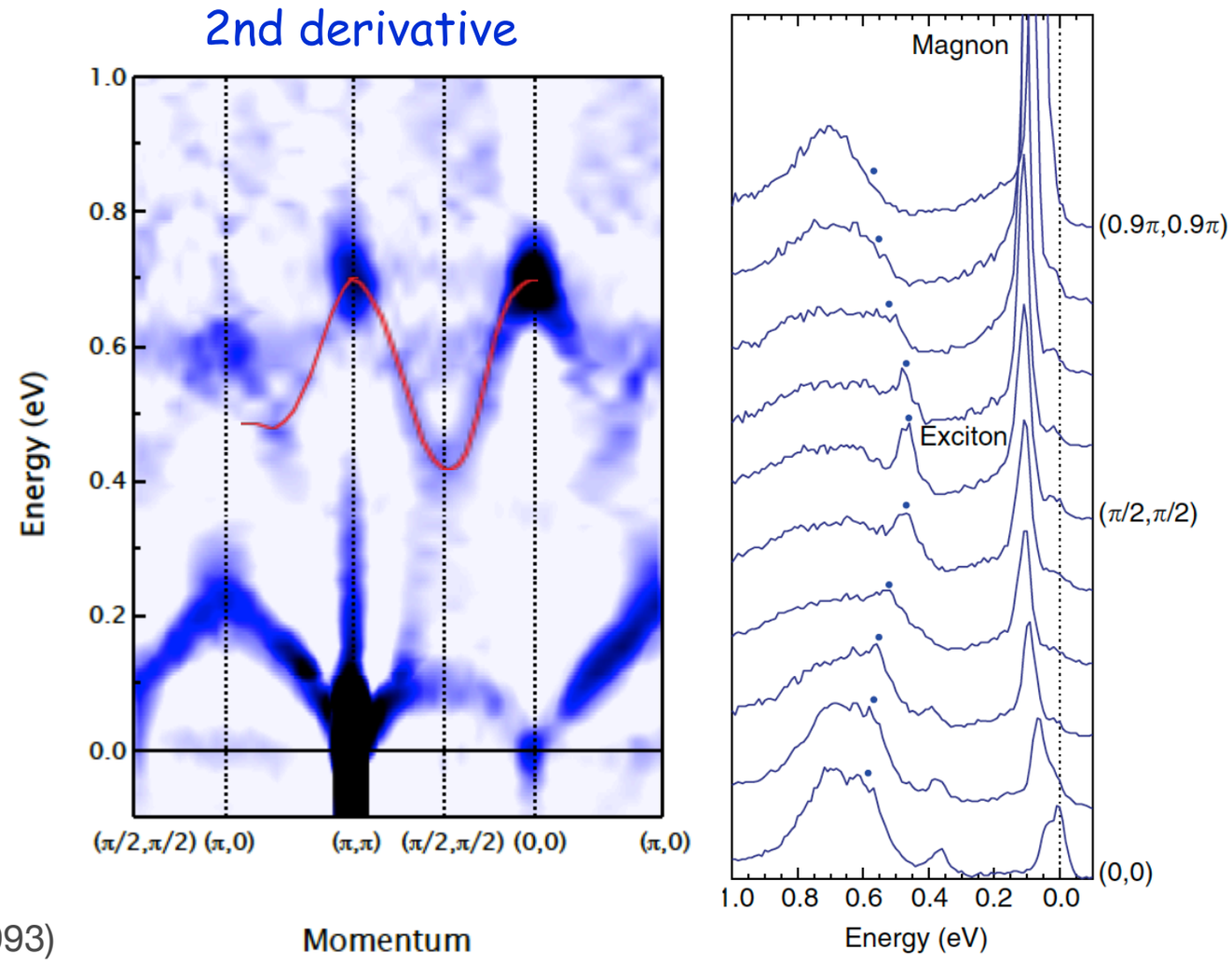

J. Kim & BJK et al. Nature Comm. (2014)

Fractional excitations

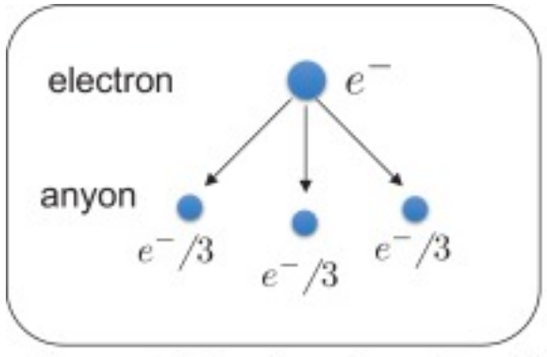

(a) $\nu = 1/3$ fractional quantum Hall

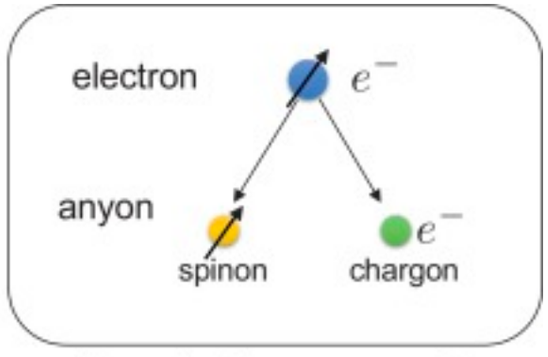

(b) spin-charge separation

Spin-charge separation

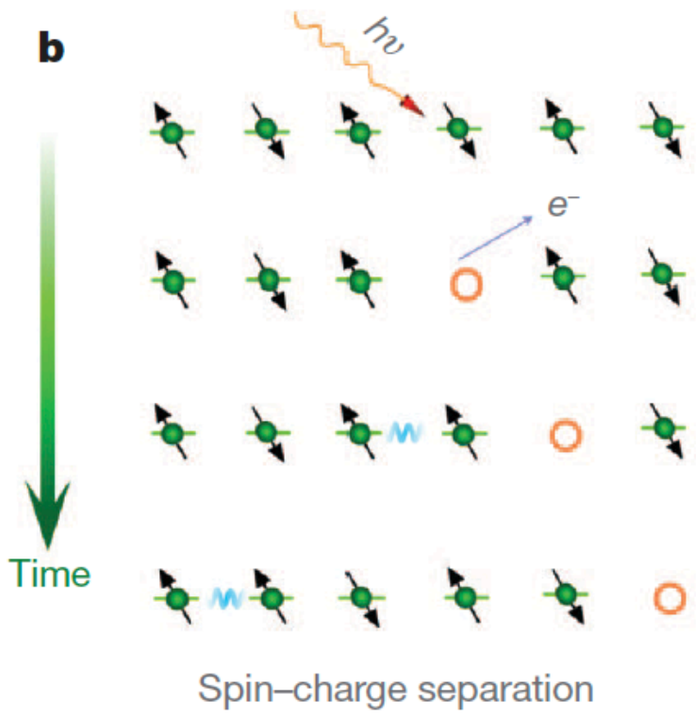

1D chain structure in Sr_2CuO_3

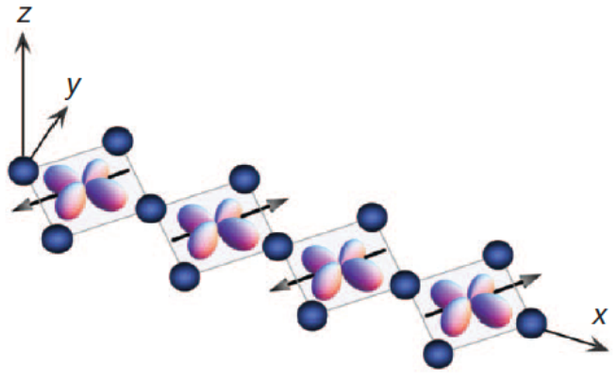

ARPES

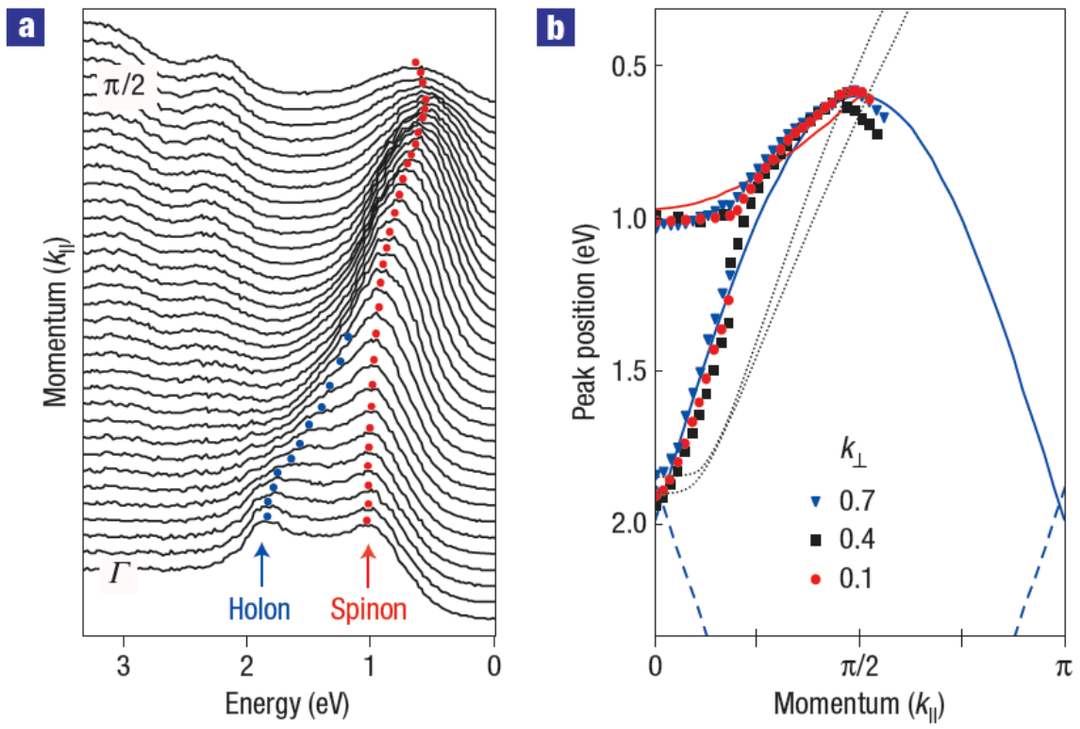

INS

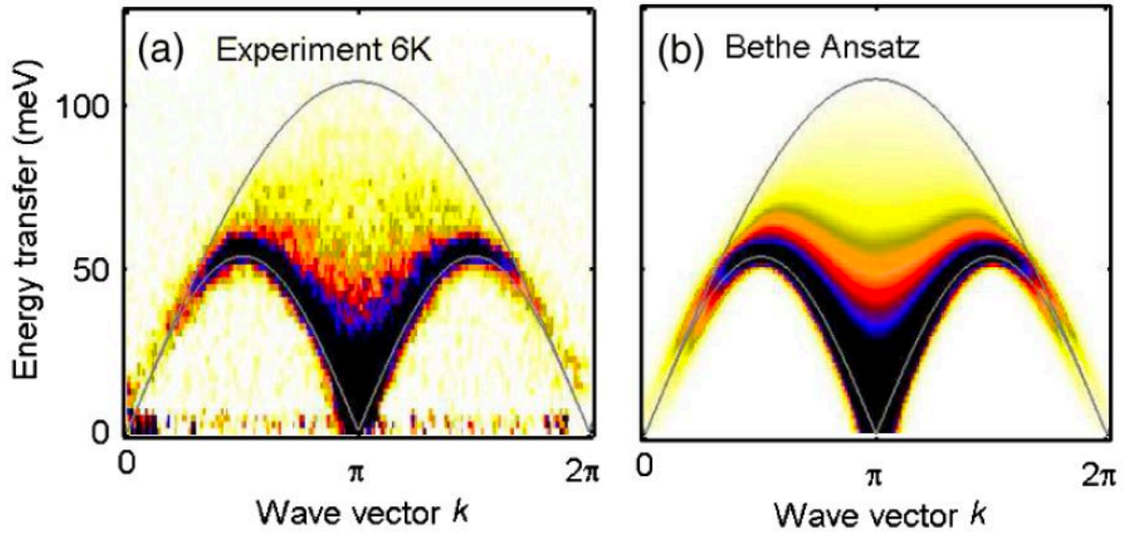

C. Kim et al. PRL (1996)
BJK, C. Kim et al. Nature Phys. (2006)

Spin-charge separation

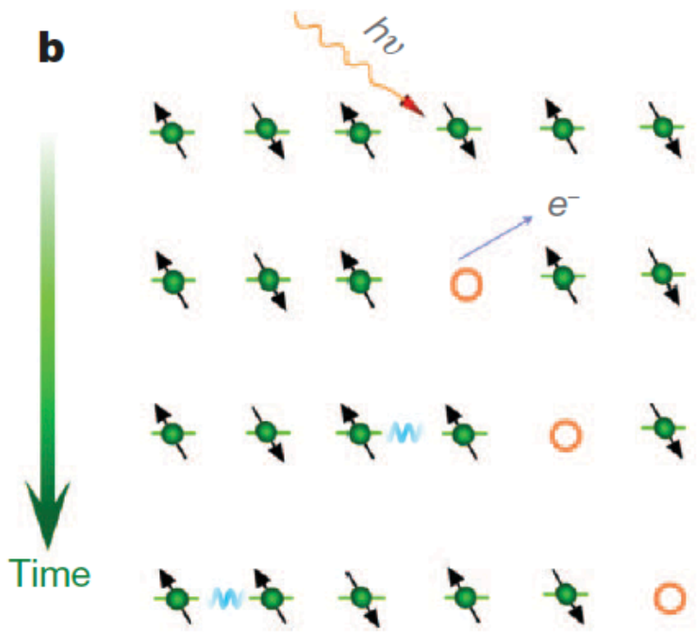

Spin–charge separation

Spin-orbital separation

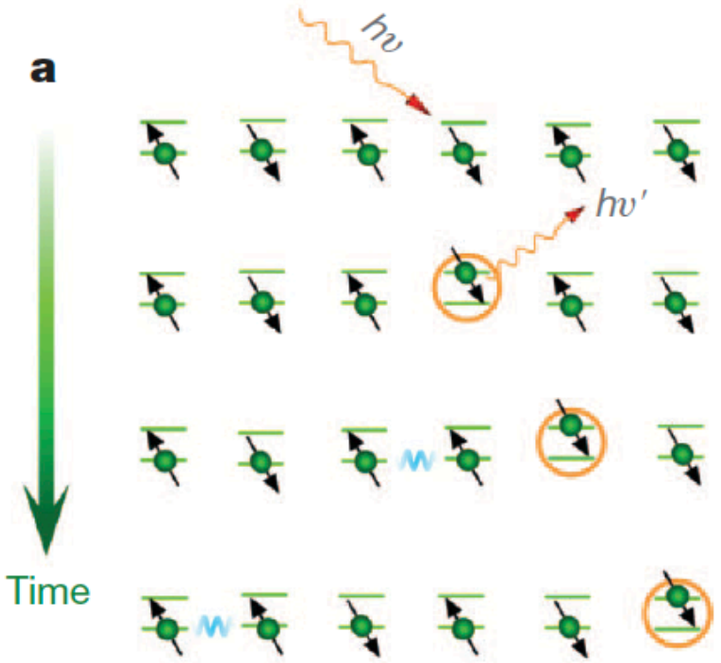

Spin–orbital separation

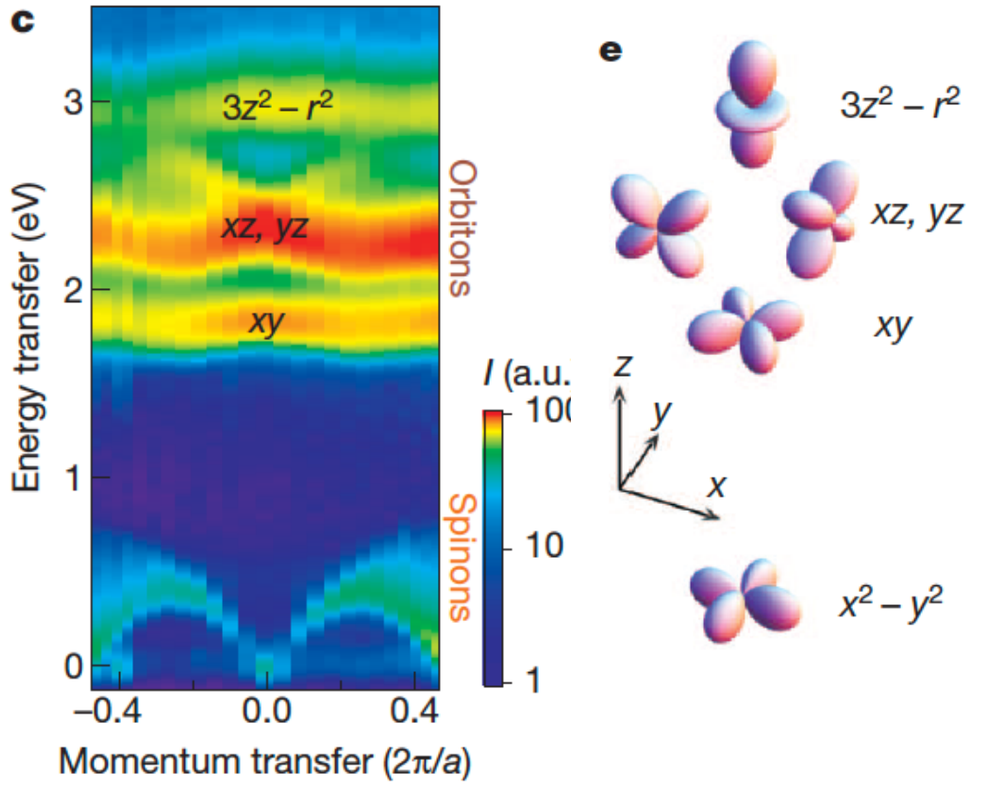

J. Schlappa et al. Nature (2012)

Spin-charge separation

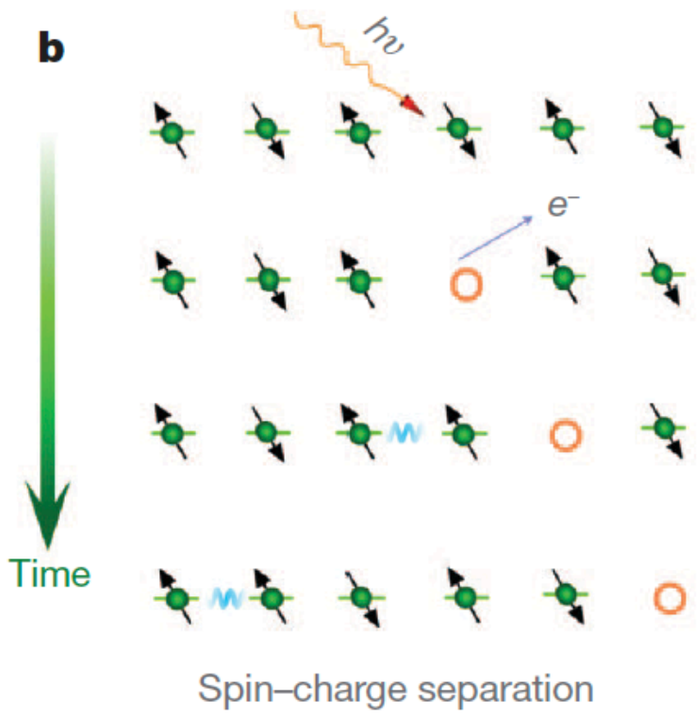

Spin–charge separation

Spin-orbital separation

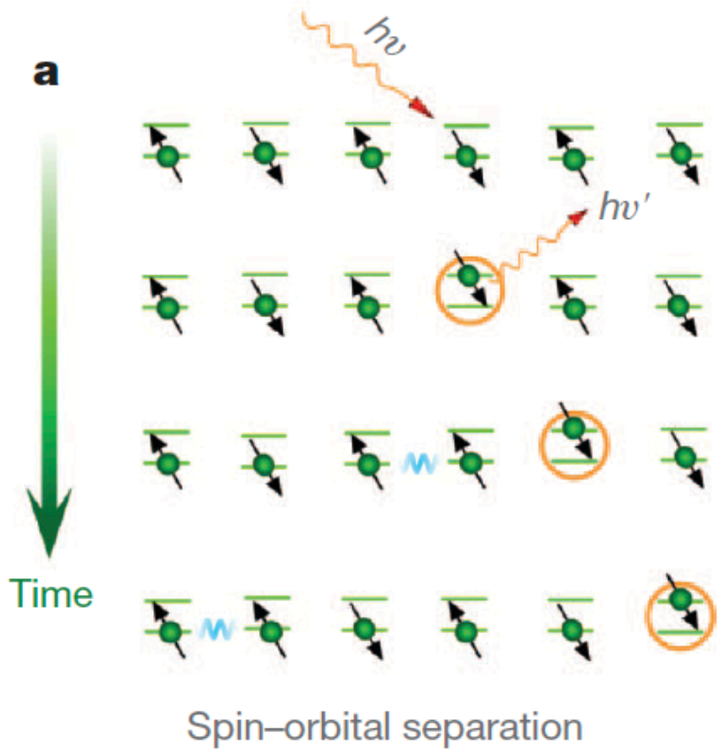

Spin–orbital separation

Spinon-orbiton continuum

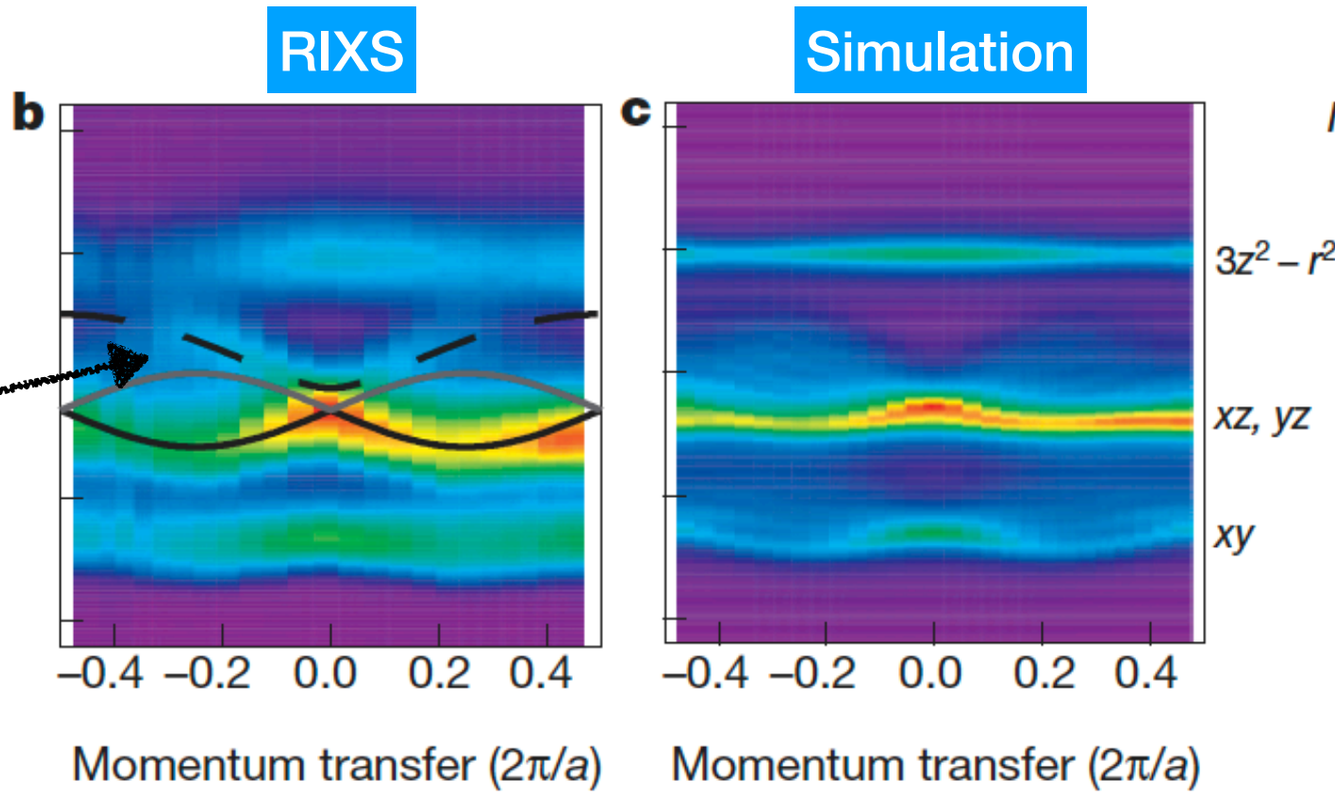

J. Schlappa et al. Nature (2012)

Recent theoretical proposals

Majorana fermions in Kitaev spin liquid

Spins fractionalize into Majorana fermions and emergent gauge fluxes

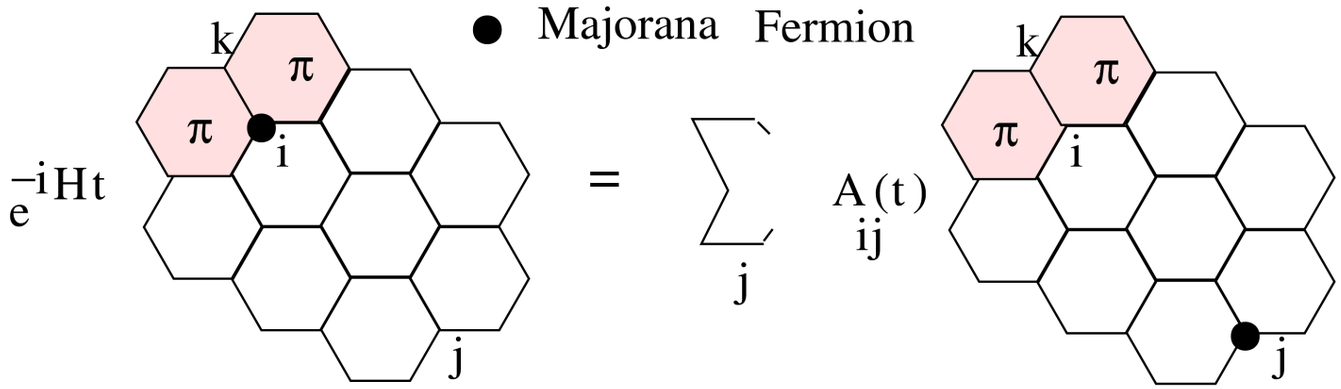

INS: dominated by static flux excitations

Raman scattering: two Majorana excitations but only at q=0

RIXS: Majorana (SC channel) and flux excitations (NSC channel)

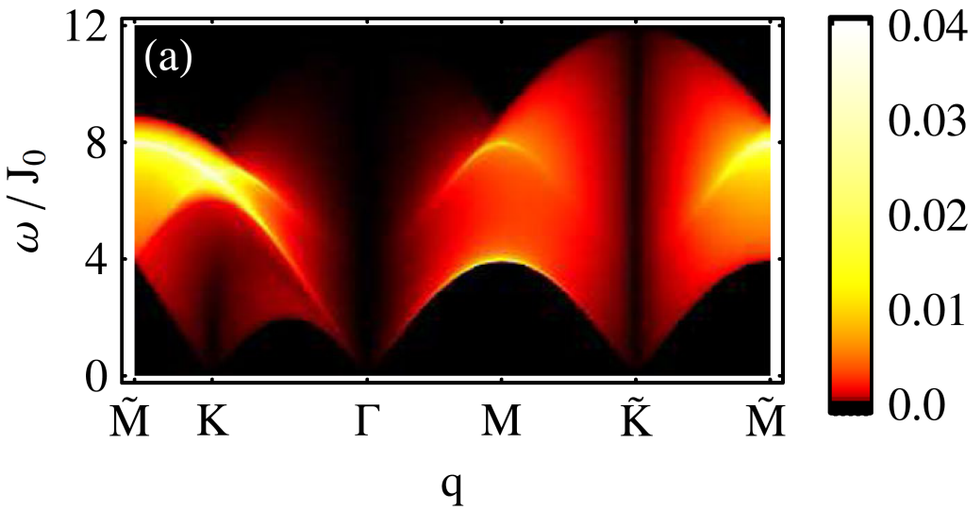

J_0~ 10-20 meV

Halasz, Perkins, van den Brink, PRL (2016)

Gauge fields

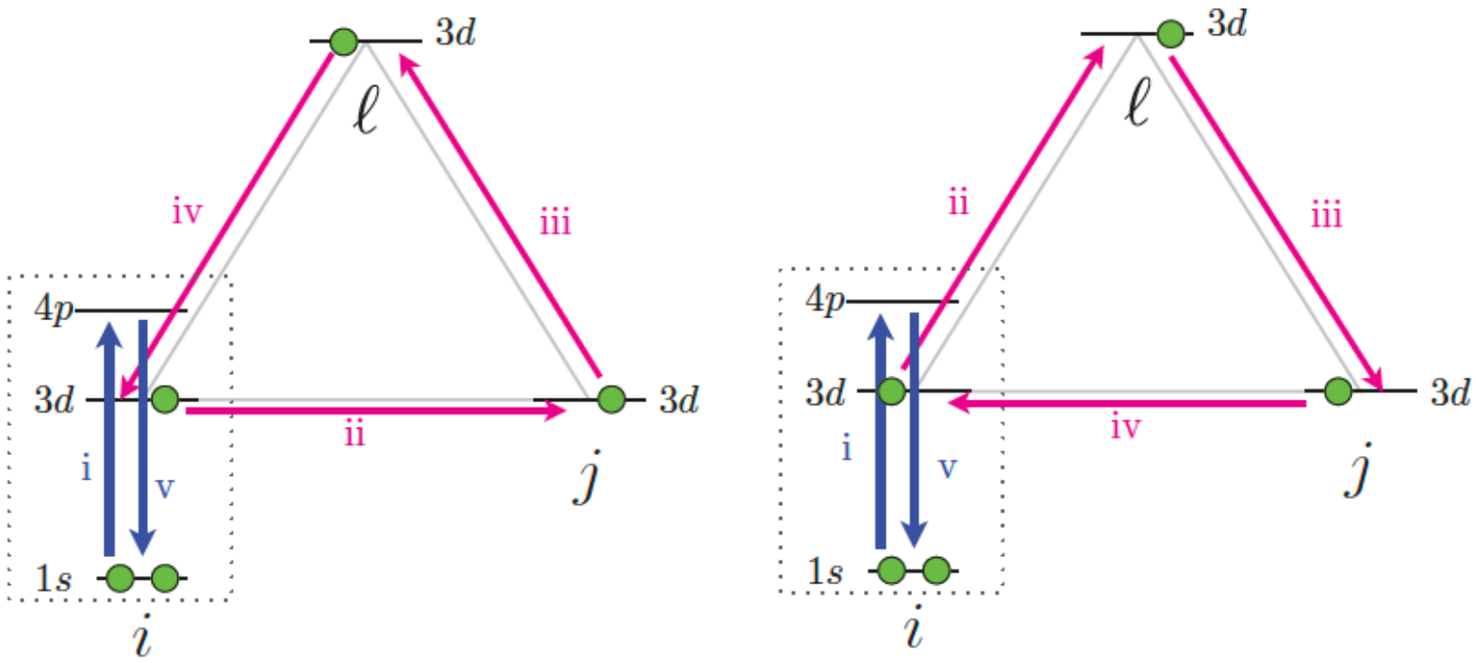

$$T^{(a)}_{\text{3-sites}} \propto \left(c^\dagger_{is}(J^\dagger)^\beta_{sp}c_{ip}\right)(t_{i\ell}c^\dagger_i c_\ell)(t_{\ell j}c^\dagger_\ell c_j)(t_{ji}c^\dagger_j c_i)\left(c^\dagger_{ip'}J^\alpha_{p's'}c_{is'}\right)$$
$$= \text{tr}\{J^\alpha(J^\dagger)^\beta\}t_{i\ell}t_{\ell j}t_{ji}\,\text{tr}\{\chi_\ell\chi_j\tilde{\chi}_i\}$$
$$= N^{\alpha\beta}t_{i\ell}t_{\ell j}t_{ji}[2i\mathbf{S}_\ell\cdot(\mathbf{S}_j\times\mathbf{S}_i)+\cdots], \qquad (9)$$

In a U(1) spin liquid, spin chirality translates into

$$\sim \langle i|b(\Delta\mathbf{k},\Delta\omega)b(\mathbf{0},0)|i\rangle + \cdots$$

where b is effective magnetic field associated with the emergent gauge boson

W.-H. Ko and P. A. Lee, PRB (2011)

Summary

- RIXS is a powerful tool sensitive to charge, spin, and orbital degrees of freedom.

- As such, it is useful for measuring spin-wave (magnon) dispersions, but can also be used to detect more exotic particles not readily measured by conventional probes.